

AMERICAN UNIVERSITY OF BEIRUT

PYROLYSIS OF WASTE POLYETHYLENE INTO FUEL: A
TWO-STAGE PROCESS MODELING STUDY

by
YOUSSEF CHAFIC SAFADI

A thesis
submitted in partial fulfillment of the requirements
for the degree of Master of Engineering
to the Department of Mechanical Engineering
of the Faculty of Engineering and Architecture
at the American University of Beirut

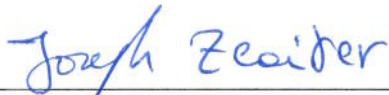
Beirut, Lebanon
October 2012

AMERICAN UNIVERSITY OF BEIRUT

PYROLYSIS OF WASTE POLYETHYLENE INTO FUEL: A
TWO-STAGE PROCESS MODELING STUDY

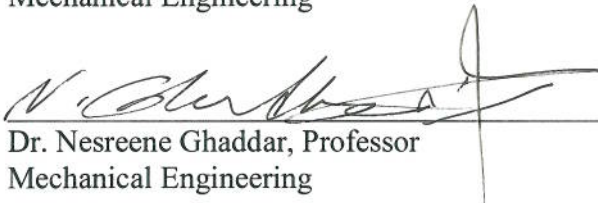
by
YOUSSEF CHAFIC SAFADI

Approved by:



Dr. Joseph Zeaiter, Assistant Professor
Mechanical Engineering

Advisor



Dr. Nesreene Ghaddar, Professor
Mechanical Engineering

Member of Committee



Dr. Kamel Ghali, Associate Professor
Mechanical Engineering

Member of Committee

Date of thesis defense: October 24, 2012

AMERICAN UNIVERSITY OF BEIRUT

THESIS RELEASE FORM

I, Youssef Chafic Safadi

authorize the American University of Beirut to supply copies of my thesis/dissertation/project to libraries or individuals upon request.

do not authorize the American University of Beirut to supply copies of my thesis/dissertation/project to libraries or individuals for a period of two years starting with the date of the thesis/dissertation/project defense.

Signature

Date

ACKNOWLEDGMENTS

I would like to thank first and utmost my advisor Dr. Joseph Zeaiter for this opportunity to conduct this research. His continuous advice, guidance and help, on many levels, have been invaluable to conducting research in a completely new area of study to me. I am grateful to have been a part of the Applied Energy program and been given this exquisite opportunity of conducting such niche research. On that note, I would like to thank Dr. Nesreen Ghaddar and Dr. Kamel Ghali for their support, guidance and care throughout my Master's Degree.

I would like to thank my family, friends and colleagues for their continuous moral support throughout my Master's degree and during my research. It was essential to keep me moving forward.

AN ABSTRACT OF THE THESIS OF

Youssef Chafic Safadi for Master of Engineering
Major: Mechanical Engineering, Applied Energy

Title: Pyrolysis of Waste Polyethylene into Fuel: A Two-Stage Process Modeling Study

Plastic waste is an ever growing problem due to the fact that it does not degrade easily unlike organic materials. Pyrolysis is one effective method to transform waste (biomass, municipal waste, plastic waste among others) into fuel. Researchers, thus far, have been developing tools to understand in depth the mechanisms that drive the thermal or catalytic degradation of polymer waste and to predict the kinetics involved in such processes as well as product distributions.

This work aims at developing an efficient pyrolysis prediction system for the process of converting waste high density polyethylene (HDPE) into fuel. The main objectives are concentrated towards the development of a computationally efficient, high fidelity model that describes the thermal degradation of the polymer with high product distribution detail. A combined model with two modeling frameworks has been suggested. It consisted of a Lumped-Empirical model approach whose aim is to depict lumps of products of the first stage (gas, low molecular weight products, waxes, etc.) and a Population-Balance model that tracks the latter products following their mechanistic reactions and depicts their carbon-chain length distribution. A pathway model was developed specifically for this purpose and was based on literature data along with parameter estimation for the kinetic rate constants.

The model tracked 181 species showing good fit with literature data. The model has the advantage of being less computationally demanding relative to existing techniques for carbon-chain length tracking of HDPE pyrolysis products.

CONTENTS

ACKNOWLEDGMENTS.....	ii
LIST OF ILLUSTRATIONS	vi
LIST OF TABLES	vii
LIST OF ABBREVIATIONS	viii
Chapter	
1. INTRODUCTION.....	1
1.1 Thermal Decomposition.....	3
1.2 Catalytic Decomposition	5
1.3 Thesis Objectives	6
2. LITERATURE REVIEW.....	8
2.1 Power Law Models.....	8
2.2 Lumped-Empirical Model	13
2.3 Population-Balance-Based Modeling.....	18
2.4 Functional-Group, Depolymerization, Vaporization, Cross-linking Model (FG-DVC).....	24
2.5 Model findings	25
3. A TWO STAGE MODELing APPROACH FOR THE POLYETHYLENE PYROLYSIS PROCESS	26

3.1 Modeling the Two-Stage Pyrolysis Process.....	27
3.1.1 Modeling the First Stage	27
3.1.2 Modeling of the Second Stage	32
3.1.2.1 Product Yields from the Second Stage Model.....	39
4. MODEL ASSEMBLY AND SOLUTION	41
4.1 Model Assembly	41
4.2 Model Solution.....	42
4.3 Discussion	52
5. CONCLUSIONS AND RECOMMENDATIONS	54
5.1 Conclusions	54
5.2 Recommendations	55
REFERENCES	56

ILLUSTRATIONS

Figure

1: Time evolution of the lumps of products from the pathway model	31
2: Comparison between model and literature results of condensable alkene yields for 125,000 M_{w0} HDPE pyrolysis at 420 °C after 90 minutes	43
3: Comparison between model and literature results of condensable alkene yields for 125,000 M_{w0} HDPE pyrolysis at 420 °C after 150 minutes	44
4: Comparison between model and literature results of condensable alkane yields for 125,000 M_{w0} HDPE pyrolysis at 420 °C after 90 minutes	45
5: Comparison between model and literature results of condensable alkene yields for 125,000 M_{w0} HDPE pyrolysis at 420 °C after 150 minutes	46
6: Comparison between model and literature results of gaseous alkane yields for 125,000 M_{w0} HDPE pyrolysis at 420 °C after 90 minutes	47
7: Comparison between model and literature results of gaseous alkane yields for 125,000 M_{w0} HDPE pyrolysis at 420 °C after 150 minutes	47
8: Comparison between model and literature results of gaseous alkene yields for 125,000 M_{w0} HDPE pyrolysis at 420 °C after 90 minutes	48
9: Comparison between model and literature results of gaseous alkene yields for 125,000 M_{w0} HDPE pyrolysis at 420 °C after 150 minutes	48
10: Comparison between model and literature time evolution results of Oil yields for 125,000 M_{w0} HDPE pyrolysis at 420 °C	49
11: Comparison between model and literature time evolution results of Gas yields for 125,000 M_{w0} HDPE pyrolysis at 420 °C	50
12: Comparison between model and literature time evolution results for =C ₉ , =C ₁₄ and =C ₁₈ for 125,000 M_{w0} HDPE pyrolysis at 420 °C	51

TABLES

Table

1: Models of kinetic functions $f(\alpha)$	10
2: Summary of Power-Law models in the literature	11
3: Summary of some Lumped-Empirical models in the literature.....	13
4: Estimated rate constants with their corresponding standard deviations	30
5: Rate parameters for mechanistic reactions' rate constants	38
6: Product formation from different reaction types	39

ABBREVIATIONS

C_m : stoichiometric coefficient for partitioning mass between degradation products

D_m : m^{th} moment of dead chains

D_n : dead chain of length n

e_f : number of bonds not able to undergo bond fission

e_t : number of monomer units without abstractable mid-chain hydrogen atoms

f : smallest fraction of branched species mass breaking off

i : chain length in monomer units

j : chain length in monomer units

k_{bbf} : rate constant for the backbiting reaction forming a mid-chain radical

k_{bbr} : rate constant for the backbiting reaction forming an end-chain radical

k_{bs} : β -scission rate constant

k_c : radical recombination rate constant

k_d : disproportionation rate constant

k_{dp} : depropagation rate constant (end-chain β -scission)

k_f : chain fission rate constant

k_{fb} : rate constant for fission at a branch point

k_{fs} : rate constant for fission at a specific location along a polymer chain

k_p : propagation rate constant

k_{ra} : radical addition rate constant

k_{tr} : chain transfer rate constant

$k_{tr,e}$: chain transfer rate constant for the formation of a mid-chain radical from an end-chain radical

$k_{tr,m}$: chain transfer rate constant for the formation of an end-chain radical from a mid-chain radical

m : the m^{th} moment of species

M : symbol for monomer

N : chain length in monomer units

r_s : specific radical of length s

s : length of a specific radical in monomer units

x : chain length in monomer units

y : chain length in monomer units

Re_i : end-chain radical of length i

Re^m : m^{th} moment of end-chain radicals

Rm_i : mid-chain radical of length i

Rm^m : m^{th} moment of mid-chain radicals

Lw : light-wax range products

Hw : heavy-wax range products

P : initial polymer

G : gas-range products

CHAPTER 1

INTRODUCTION

Plastics have been around for some time. They can be traced back to 1847. However, their commercialization was onset after the shortage in supply of natural rubbers during the Second World War. Plastics are light weight, easily molded, highly durable, and low cost materials¹. This means that plastics have a wide range of applications. They can be used to make plastic bags, bottles, accessories, chairs, tables and many more. Consequently, more plastic wastes are ever being produced. In Lebanon and according to a major municipal waste collection company (Sukleen), it is reported that 109500 tons of plastic waste per year are being collected of which only 3-4% are recovered. The non-recycled figures are estimated to be 16800 tons/year. This raises serious environmental concerns as landfill areas are shrinking more and more and the fact that plastic wastes are non-biodegradable makes them reside in landfills for long periods of time taking up valuable land space.

Alongside landfilling, incineration of plastic waste, known as quaternary recycling, is an economically viable route to get rid of plastic wastes and use their high calorific value for energy generation. This method however is largely questioned due to emissions of toxic compounds such as dioxins and furans². Bringing plastic waste back into the consumption cycle and taking some of the load from landfills necessitates the development of far more advanced recycling technologies; one of the most promising types is tertiary recycling.

Mechanical recycling of plastics consists of separation by resin, cleansing to remove contaminants, grinding and crushing to reduce the plastic particle size, and finally heat extruding and reprocessing into new plastic yields of similar mechanical properties. Thermosets such as urea-formaldehyde resins (UF), melamine-formaldehyde resins (MF), phenol-formaldehyde resins (PF), epoxy resins, unsaturated polyesters, alkyd resins and polyurethanes cannot be heat extruded or remolded; therefore, limiting this type of recycling to thermoplastics that include Polyethylene (PE), Polypropylene (PP), Polystyrene (PS), Polyvinyl Chloride (PVC) and Polyethylene Terephthalate (PET). Given that plastic waste is composed of mixed species, mechanical recycling is limited in the sense that the presence of even the smallest amounts of a polymer in the matrix of the desired polymer to be recycled might dramatically alter the properties of the latter, thus, rendering it useless in its original application. Over and above, the different coloring in the end products of plastic waste would usually yield in an unwanted grey color to the recycled plastic³.

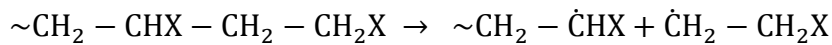
Pyrolysis, a tertiary recycling technique, is the decomposition of organic material at high temperatures in the absence or lack of oxygen³. It involves thermally degrading plastics at high or moderate temperatures back to feedstock material. This feedstock then can be used in a chemical production process or can be upgraded to be used further as a fuel similar to that derived from crude oil. Thermal degradation is generally carried out at high temperatures and catalytic degradation (incorporating a catalyst) at lower temperatures. This type of recycling is of particular interest since it does not require preprocessing of the plastic waste such as cleansing, separation by color or sorting.

1.1 Thermal Decomposition

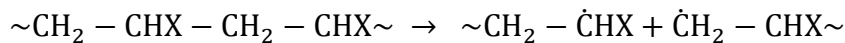
Thermal decomposition is the degradation of polymers in the absence of oxygen or in a very low oxygen medium. The thermal decomposition of plastic waste such as polyethylene and polypropylene alongside other addition polymers, would lead to a wide range of products². In order to control or narrow this wide range of product yield, the reaction variables ought to be controlled such as polymer feed, reactor type and operation, and more importantly temperature¹. In order to understand better the thermal decomposition process, we must understand, at a molecular level, how the polymer chains decompose and propagate throughout the reaction. A general mechanism was proposed by Stivala et al⁴ for the thermal degradation of addition polymers. Their mechanism entails:

- Initiation:

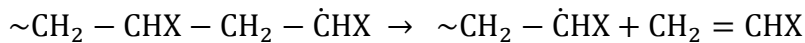
- End-chain scission



- Random scission

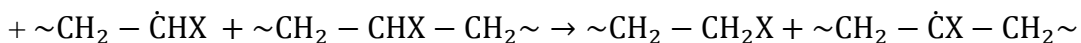
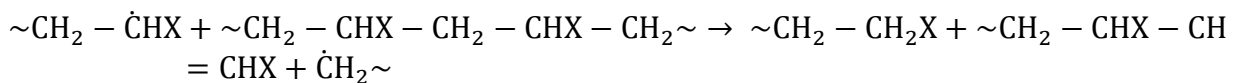


- Depropagation

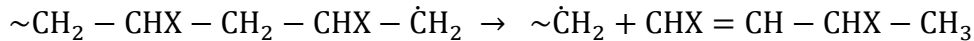


- Hydrogen chain transfer reactions:

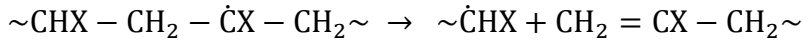
- Intermolecular transfer reaction



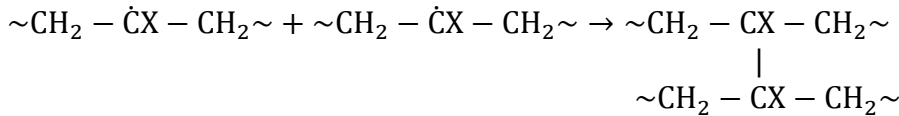
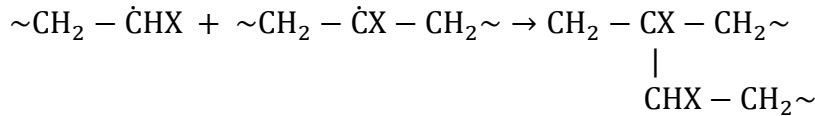
- Intramolecular transfer reaction



- β -Cleavage of secondary radicals:

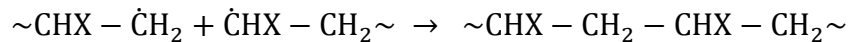


- Branching:

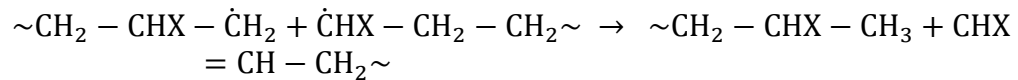


- Termination:

- Bimolecular coupling



- Disproportionation



It should be noted that other reactions, such as cyclization, aromatization, isomerizations and recombination, might take place throughout this process. This usually increases the degree of branching while the length of the polymer chain is reduced¹.

In order to understand the degradation mechanisms, we need to discern some figures. A carbon-carbon bond has an energy level of 83 kcal/mole while a carbon-hydrogen bond has 94 kcal/mole on average. This is precisely why the initiation reaction in most polyolefins, such as polyethylene, begins with backbone cleavage or breaking of the backbone molecules since the

energy required to break a carbon-carbon bond is less than the energy required to break a carbon-hydrogen bond. Primary radicals are thus generated. This primary radical can undergo hydrogen abstraction from a nearby molecule to form two products: a stable product due to the saturation of a newly found carbon-hydrogen bond from the hydrogen abstracted and a secondary radical, which can be formed also from a hydrogen shift from the primary radical. This primary radical can further undergo a beta scission to form an unsaturated product⁵.

1.2 Catalytic Decomposition

The catalytic cracking of polymeric materials is basically a thermal degradation process that incorporates the use of a catalyst. It surpasses its thermal counterpart due to its lower cracking temperatures, activation energies and quality of the pyrolysis fuel or specificity of the product. The catalyst selectivity, pore size and shape, and the type of catalyst site (e.g. Brönsted or Lewis acid site) play a major role in the degradation process. The degradation mechanism involving a catalyst is fairly straight forward. The feed first vaporizes due to the hot catalyst surface then forms carbon ions, also known as carbocations. Carbenium ions, which belong to the carbocation family, are formed from either an olefin or paraffin. When the Brönsted acid site of the catalyst donates a proton to an olefin, a carbenium ion is generated. Likewise, when the Lewis acid site of the catalyst removes electrons to form paraffin, a carbenium ion is formed. Thus, the Brönsted and Lewis acid sites of the catalyst are an important property to be taken into consideration in studying the catalytic degradation mechanisms⁶.

The most investigated catalysts used in the petrochemical industry, are silica alumina⁷⁻¹⁰, ZSM-5¹¹⁻¹⁴, Y-type zeolite^{15,16}, Beta zeolite^{17,18} and MCM-41¹⁹⁻²¹. These catalysts, among others, are capable of altering the degradation mechanism and actively selecting the evolved

species to give a certain product or range of products. An in-depth review of various catalysts can be found in Aguado et al².

1.3 Thesis Objectives

This work aims at developing an efficient pyrolysis prediction tool to simulate the process of converting plastic waste into fuel. The main objectives are concentrated towards the development of a high fidelity mechanistic model that describes the mechanisms that take place during the thermal degradation of the polymer. A two-stage modeling approach is adopted to model the product distribution according to the carbon chain length.

In the first stage, the modeling of the pyrolysis of polyethylene is lumped into a set of specific products of lower molecular weight/chain length; afterwards, the second stage consists of the pyrolysis of the lumped products into lower molecular weighted products, with high details of the chain length product distribution. This hybrid modeling approach comprises of a Lumped-Empirical model coupled with a Population-Balance model with kinetic parameters estimated from available data in the literature. The following objectives are set for this work:

- Define a lumped empirical scheme over which the pyrolysis of HDPE will take place
- Develop a model based on population balances to govern reactions at the mechanistic level
- Combine the aforementioned models to simulate the waste HDPE pyrolysis process

This hybrid approach was developed with the purpose of giving new insights on polymer pyrolysis with an emphasis on computational efficiency, being achieved by the relatively low number of differential equations that governs both models in comparison to current methods that track pyrolysis products according to their carbon-chain length. This new

approach also offers a new methodology to solve population-balance based models without using any lumping schemes for the population-balance equations for their solution. This is of great significance because this methodology might be a springboard for future development of population-balance based models with exceptional product-spectrum precision after the inclusion of known aspects of polymer structure, such as branching and weak bonds, and known aspects of pyrolysis, such as cyclization and aromatization.

CHAPTER 2

LITERATURE REVIEW

Having a mathematical model that can predict product distributions is of great value to help understand process limitations and identify areas for improvements. Besides, computer-aided simulations can be run in a much faster time as opposed to conducting experiments and carrying out laboratory analysis. Further, modeling the thermal degradation kinetics would help optimize and improve the pyrolysis process in terms of product quality, energy and time.

There have been mainly three approaches to model the thermal degradation process. These can be listed as: Power Law models, Lumped-Empirical models, and Population-Balance models.

2.1 Power Law Models

In this type of modeling, the rate or degree of conversion of the polymer in the thermal degradation process is expressed in terms of two functions. The rate of reaction is expressed as

$$\frac{d\alpha}{dt} = k(T)f(\alpha)$$

where $k(T)$ is the rate constant and $f(\alpha)$ is a function of conversion that expresses the type of reaction. Also, the rate can be written as:

$$k(T) = A\exp(-E/RT)$$

Knowing that:

$$\frac{d\alpha}{dt} = \frac{d\alpha}{dT} \frac{dT}{dt} = \frac{d\alpha}{dT} \beta$$

where A, E, R, T, and β are the pre-exponential constant, activation energy, universal gas constant, absolute temperature and heating rate respectively.

This after substitution and rearrangement gives:

$$\frac{d\alpha}{f(\alpha)} = \frac{A}{\beta} \exp(-E/RT) dT$$

Setting $G(\alpha) = \int_0^\alpha \frac{d\alpha}{f(\alpha)}$ and integrating gives:

$$\ln G(\alpha) = \ln \frac{AE}{R} - \ln \beta + \ln p(x)$$

Such that $p(x) = \frac{e^{-x}}{x} - \int_x^\infty \frac{e^{-x}}{x}$ where $x=E/RT$. Various solutions for the function $p(x)$

were proposed in the literature as listed below,

- Doyle's approximation²²: $\ln p(x) = -5.3305 + 1.052x$. This gives:

$$\ln \beta = \ln \frac{AE}{R} - \ln G(\alpha) + -5.3305 + 1.052x$$

- Friedman method²³:

$$\ln \frac{d\alpha}{dt} = \ln \beta \frac{d\alpha}{dT} = \ln[Af(\alpha)] - \frac{E}{RT}$$

- Coats-Redfern method²⁴:

$$\ln \frac{G(\alpha)}{T^2} = \ln \left[\frac{AR}{\beta E} \left(1 - \frac{2RT}{E} \right) \right] - \frac{E}{RT}$$

- Flynn-Wall-Ozawa method^{25,26}: $\ln p(x) = -2.315 - 0.4567x$.

After substitution the equation becomes:

$$\ln \beta = \ln \frac{AE}{RG(\alpha)} - 2.315 - 0.4567 \frac{E}{RT}$$

- Kissinger-Akahira-Sunrose method^{27,28}: Based on the Coats-Redfern

approximation where $p(x) = \frac{e^{-x}}{x^2}$ such that

$$\ln \frac{\beta}{T^2} = \ln \frac{AR}{Eg(\alpha)} - \frac{E}{RT}$$

When the left hand side in the above equation is plotted against $1/T$, the activation energy can be found from the slope of the line for a fixed conversion α ²⁶. As for $f(\alpha)$, it represents a function of the kinetic model. It may be written in a general form of $f(\alpha) = (1-\alpha)^n \alpha^m [-\ln(1-\alpha)]^p$ where m and p are exponents and n is the order of reaction. An assessment of the various models proposed was done by Brems et al²⁹. The latter research states that low heating rates tend to overestimate the activation energy and that equations of first and second order tend to be in agreement with the activation energies found in the literature. The following table describes some of the models found in the literature³⁰:

Table 1: Models of kinetic functions $f(\alpha)$

Model	$f(\alpha)$
Phase boundary – controlled reaction (contracting area)	$(1 - \alpha)^{1/2}$
Phase boundary – controlled reaction (contracting volume)	$(1 - \alpha)^{2/3}$
Random nucleation–Unimolecular decay law	$(1 - \alpha)$
Reaction nth order	$(1 - \alpha)^n$
Johnson–Mehl–Avrami	$n(1 - \alpha)[- \ln(1 - \alpha)]^{1-1/n}$
Two-dimensional growth of nuclei (Avrami equation)	$2[- \ln(1 - \alpha)^{1/2}](1 - \alpha)$
Three-dimensional growth of nuclei (Avrami equation)	$3[- \ln(1 - \alpha)^{2/3}](1 - \alpha)$
One-dimensional diffusion	$1/(2\alpha)$
Two-dimensional diffusion	$1/[- \ln(1 - \alpha)]$
Three-dimensional diffusion (Jander equation)	$3(1 - \alpha)^{2/3}/2[1-(1-\alpha)^{1/3}]$

Model	$f(\alpha)$
Three-dimensional diffusion (Ginstling–Brounshtein)	$3/2[(1-\alpha)^{-1/3}-1]$
n-dimensional nucleation (Avrami–Erofeev equation)	$n[-\ln(1-\alpha)^n](1-\alpha)$
Reaction of first order with autocatalysis	$(1-\alpha)(1+K_{cat}\alpha)$
Reaction of nth order with autocatalysis	$(1-\alpha)^n(1+K_{cat}\alpha)$
Prout– Tompkins equation	$(1-\alpha)^n\alpha^a$

After adopting a function that describes the degradation mechanism, the activation energy, pre-exponential constant and order of reaction can be calculated. Takeo Ozawa²⁶ suggested that the fractional weight can be expressed as a function of the fraction of a structural quantity, such as a group, a constituent, a broken bond, or any other.

The following table sums up some of the models proposed by various researchers with their findings:

Table 2: Summary of Power-Law models in the literature

Author/Researcher	Parameters investigated	Kinetic parameters found	Comments
Brems et al ²⁹	Rate of weight loss	Pre-exponential constant, Activation energy	Low values of the heating ramp overestimate the activation energy. First and second reaction orders provide good fit.
Marcillaet al ^{19,20,31,32}	Concentrations of Intermediates, volatiles	Pre-exponential constant, Activation energy, reaction order	Takes account of catalyst in model. Equations were integrated using the Euler method. Model is capable of simultaneously correlating experiments with catalysts studied.
Encinar et al ³³	Rate of weight loss	Pre-exponential constant, Activation energy	Reaction of first order As the heating rate increases, gas yield increases and vice

Author/Researcher	Parameters investigated	Kinetic parameters found	Comments
Gaoet al ³⁴	Fraction of broken bonds	Pre-exponential constant, Activation energy	versa for liquid yield. Not every bond-broken in the main chain leads to volatile products.
Sánchez-Jiménez ³⁵	Rate of weight loss	Pre-exponential constant, Activation energy	First order or nth-order $f(\alpha)$ are different from that of random scission mechanisms.
Grammelis et al ³⁰	Rate of weight loss	Pre-exponential constant, Activation energy, Coefficient of partial process contribution	Employs a coefficient that expresses the contribution of partial processes to overall mass loss.
Westerhout et al ³⁶	Rate of change of the number of each bond type	Pre-exponential constant, Activation energy	Measures intrinsic rather than apparent kinetic parameters taking into account that not every broken bond leads to volatilization. Model proved to be valid for the entire conversion range. Cannot be used above 400°C.
Aboulkas et al ³⁷	Rate of weight loss	Pre-exponential constant, Activation energy	A comparison of all available functions $f(\alpha)$ in literature was done.
Marongiu et al ³⁸	Around 60 real and lumped species and radicals	Rate constant, Activation energy	Most reactions were of zero or first order.

It should be noted that no matter what the rate is function of (conversion α , concentration, bond broken, etc.), the procedure for getting the pre-exponential constant and activation energy remains the same. Plotting the left hand side of the various equations vs. $1/T$ ought to generate a straight line. From the slope of this line, we can determine the activation energy and consequently the pre-exponential constant.

The Power Law modeling approach is direct and simple to implement. It does not require computing power and it is not time consuming. However, the mutual correlation of activation energy and pre-exponential constant makes these types of models apparent and not intrinsic because the activation energy from a model is often validated from a Thermo Gravimetric Analysis (TGA) run which is apparent and not intrinsic as pointed out by Westerhout et al³⁶. Also, this kind of modeling doesn't fully describe the mechanisms of the degradation process unless coupled to product identification equipment such as gas chromatography and/or mass spectrometry or other identification equipment. It should be also noted that unless the sample is small enough for the TGA experiment, there will be mass and heat transfer restrictions thus, affecting the fitting process of a model using thermogravimetry.

2.2 Lumped-Empirical Model

In this type of modeling, the model lumps the degradation products in a set of differential equations of mass concentrations that depict the formation of these lumps. The solution of the differential equations determines the rate constants of the various lumps formed. Many researchers have used this type of modeling as shown in the following table.

Table 3: Summary of some Lumped-Empirical models in the literature

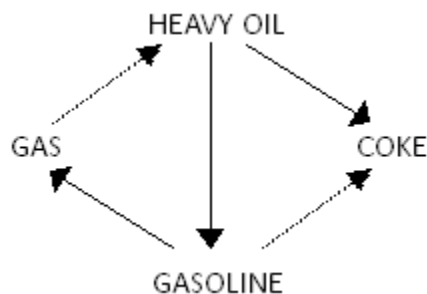
Author/Researcher	Lumping into	Kinetic parameters found	Comments
Songip et al³⁹	Concentrations of Gasoline, Gas, Coke	Rate constant, Activation energy	The kinetic parameters were evaluated by nonlinear least-squares regression
Elordi et al⁴⁰ Al-Salem et al⁴¹	Concentrations of Gas, Liquid, Wax, Aromatics, Char	Pre-exponential constant, Activation energy	High residence time affects fit.

Author/Researcher	Lumping into	Kinetic parameters found	Comments
Miskolczi et al ⁴²	Concentrations of Intermediates, Paraffin, Vinyl Olefin, Tertiary Olefin, Internal Olefin, Residue	Reaction constant	Reactions of first order. Good fit of model. Olefinic double bonds are shifted from the terminal to internal position of the carbon chain under catalysis.
Lin et al ^{10,43,44} Lin et al ⁹	Concentrations of Complex of hydrocarbon and catalyst, n/isomeric olefins and carbenium, Intermediates, paraffins, olefins, HCl, Coke/BTX	Rate constants	Differential equations were solved with Runge-Kutta algorithm in Matlab. Model incorporated activity decay function for the catalyst.
Costa et al ⁴⁵	Concentrations of Plastic mixture, solid lower molecular weight polymer, gas, light liquid fraction, heavy liquid fraction	Rate constants	All reactions are first order and irreversible. Logarithmic form of the Arrhenius equation did not display linearity thus deduced not to be the best approach for the calculation of activation energy and pre-exponential factor.

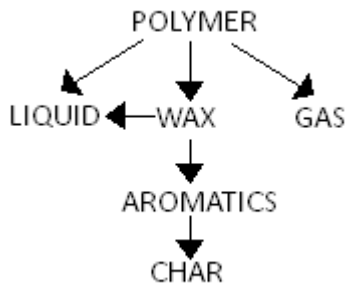
Author/Researcher	Lumping into	Kinetic parameters found	Comments
Faravelli et al ⁴⁶⁻⁴⁸	Fractions of Alkane, Alkene, and Dialkene	Rate constant, Activation energy	Rate constants of different elementary reactions were found such as β -scission, H-abstraction (intermolecular and intramolecular), Recombination and Disproportionation reactions. Primary secondary and tertiary radicals were taken into account as well as liquid and gaseous phase reactions. Schultz distribution was assumed. Numerical integration was done through an implicit multi-step Adams-Moulton method or explicit Adams algorithm. Was able to replicate the TG runs with good fit.

This approach is used to get the rate constants of the various lumps and determine their final concentration. This type of modeling is somehow limiting since it does not describe the reaction mechanisms and is limited to the proposed lumps in the model; Here are some schemes proposed by different researchers:

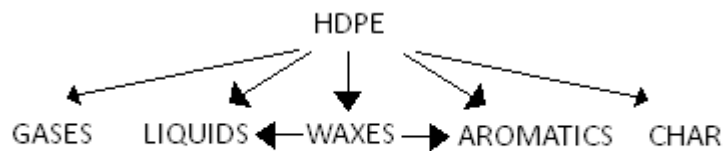
- Songip et al³⁹



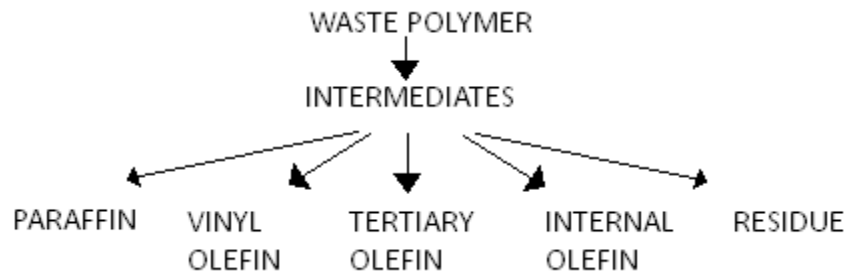
- Elordi et al⁴⁰



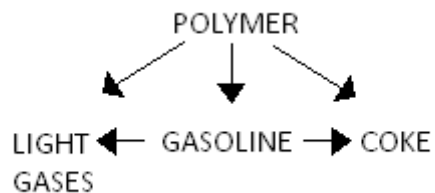
- Al-Salem et al⁴¹



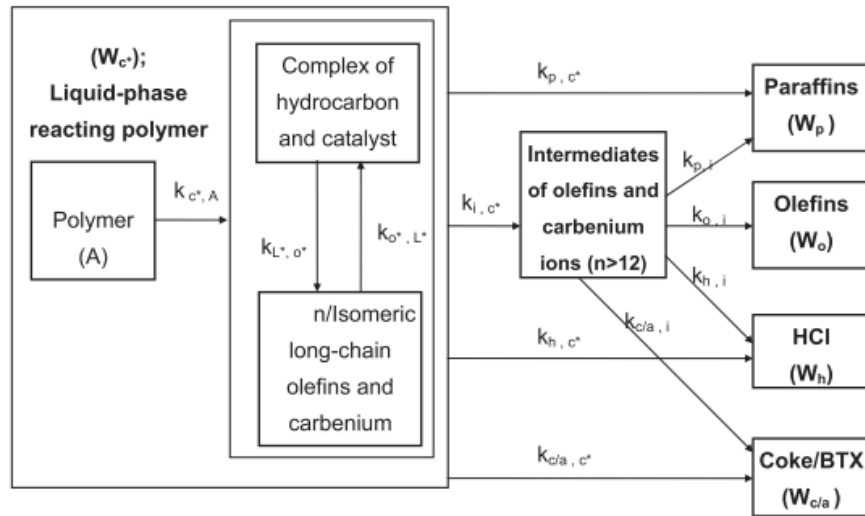
- Miskolczi et al⁴²



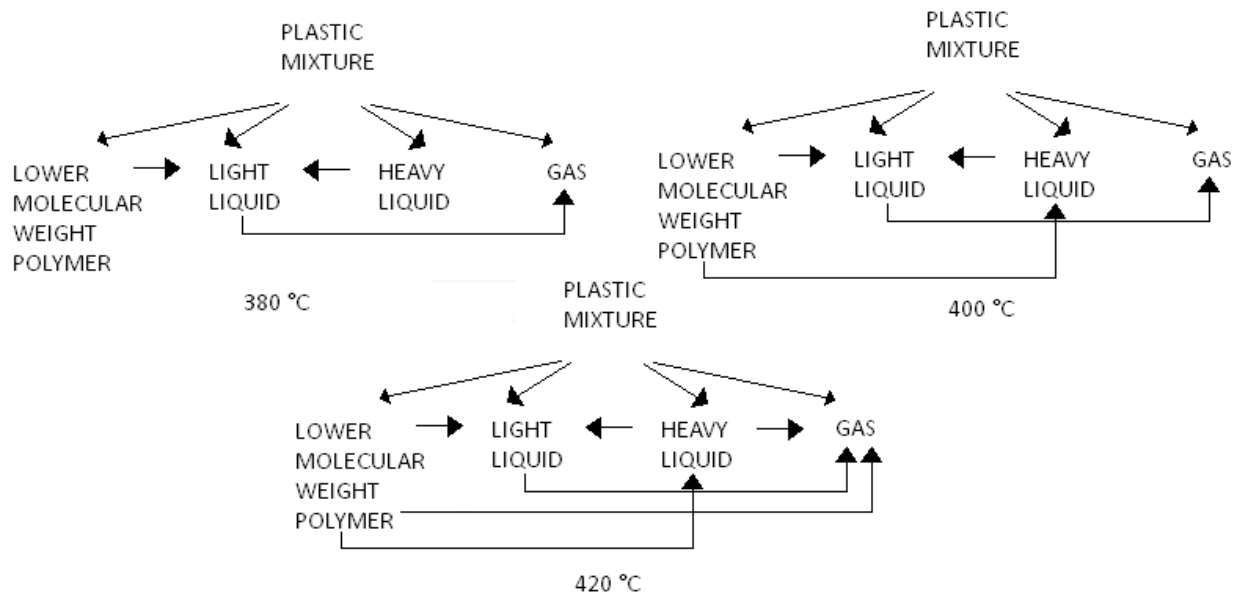
- Lin et al⁸



- Lin et al^{7,45,46}



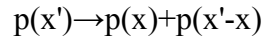
- Costa et al⁴⁵



2.3 Population-Balance-Based Modeling

Population balance equations can be used to study the thermal degradation process. Models based on them describe the evolution of the frequency distributions of polymeric chains with different molecular weights. They are employed to describe the evolution of the frequency distributions of different-sized fragments. Unit fragments can either yield random or parabolic distributions of binary daughter-products or specific distribution of products⁴⁹. Molecular-weight distributions (MWD) can be determined experimentally by gas permeation chromatography.

Population balance equations can be written for both discrete and continuous MWDs. If the MWD allows integrals to represent averages of the distribution, only then the continuous kinetics are valid. Let us consider a random degradation of a polymer P with molecular weight x' . Then it will degrade into two fragments of lower molecular weights x and $x'-x$ according to the following equation:



The governing equation is then⁵⁰:

$$\frac{\partial p(x, t)}{\partial t} = -k(x)p(x, t) + 2 \int_x^{\infty} k(x')p(x', t)\Omega(x, x') dx'$$

where $\Omega(x, x')$ is the stoichiometric kernel that determines the distribution of scission products and $k(x)$ is the rate coefficient prone to have the form:

$$k(x) = k_p(x - x_0)^p$$

where x_0 is the smallest molecular weight reactant that can crack. The general form of the stoichiometric kernel is:

$$\Omega(x, x') = x^m(x' - x)^m \Gamma(2m + 2) / [\Gamma(m + 1)^2 (x')^{2m+1}]$$

This can be reduced to $\Omega(x, x') = 1/x'$ in the case of totally random fragmentation; where $m=0$ and $m=\infty$ correspond to random and midpoint chain scission, respectively. In the case of proportioned, specific product release, or depolymerization, the stoichiometric kernel can be written in the form of a Dirac Delta function: $\Omega(x, x') = \delta(x - bx')$ where b is fraction number.

The gamma function is defined by applying Stirling's formula as:

$$\Gamma(x) \approx (2\pi/x)^{1/2} x^x \exp(-x)$$

There are many ways to solve the integrodifferential population balance equations. Moments' method, similarity method, numerical methods or any other method can be used to solve the aforementioned balance equations. Sterling et al⁵¹ discusses various solutions of integrodifferential population balance equations. The most popular is to either differentiate the population balance equations to obtain a set of partial differential equations or to convert the equations into moments where the n^{th} moment is defined by:

$$p^{(n)}(t) = \int_0^{\infty} p(x, t) x^n dx$$

From here we can distinguish the following:

- Zeroth moment ($n=0$): the time-dependent total molar concentration
- First moment ($n=1$): the mass concentration
- Normalized First moment: average MW equals $p^{\text{avg}}=p^{(1)}/p^{(0)}$
- Second central moment: variance of the MWD equals $p^{\text{var}}=p^{(2)}/p^{(0)} - [p^{(\text{avg})}]^2$

- Mass average $M_w = p^{(2)}/p^{(1)}$
- Molar average $M_n = p^{avg}$
- Polydispersity index $D = M_w/M_n = p^{(2)} p^{(0)}/[p^{(1)}]^2$

$p^{(0)}$, p^{avg} , and p^{var} describe the shape characteristics of the distribution. The gamma distribution is also constructed from these three moments. It should be noted that Gaussian, Poisson, and exponential distributions are special cases of the gamma distribution. The zeroth moment alone is usually required to determine the rate coefficient from experimental data.

Applying the moment operation⁵² to the governing equation yields:

$$dp^{(j)}/dt = kc^{(j)} (1 - j)/(1 + j) - Kc^{(r+j)}$$

The moments represent the distribution:

$$p(x) = [p^{(0)}/\beta\Gamma(\alpha)]y^{\alpha-1}\exp(-y)$$

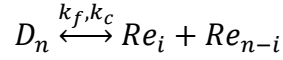
where $y = (x - x_0)/\beta$, x_0 is the minimum size of a molecule, α and β are related to the first and second moments in expressions that define the average and variance of the gamma distribution function:

$$p^{(1)}/p^{(0)} = x_0 + \alpha\beta$$

$$p^{(2)}p^{(0)} - [p^{(1)}/p^{(0)}]^2 = \alpha\beta^2$$

Kruse et al⁵³ developed a model to track the evolution of the molecular weight distribution using elementary steps to govern the moment equations. From here we can depict the elementary reactions and their corresponding moment equations as follows:

- Random fission



$$\frac{dD^m}{dt} = -k_f(2D^{m+1} - e_f D^m) + \frac{1}{2} k_c \sum_{j=0}^m \binom{m}{j} Re^j Re^{m-j}$$

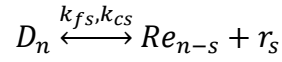
$$\binom{m}{j} = \frac{m!}{j!(m-j)!}$$

$$D^3 = \frac{2D^2 D^2}{D^1} - \frac{D^2 D^1}{D^0}$$

$$\frac{dRe^m}{dt} = 2k_f C_m (2D^{m+1} - e_f D^m) - k_c Re^m Re^0$$

$$C_m = \frac{1}{m+1}$$

- Specific Chain Fission/Radical Recombination

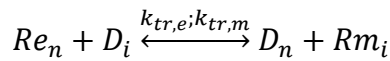


$$\frac{dD^m}{dt} = -k_{fs} D^m + k_c \sum_{j=0}^m \binom{m}{j} Re^{m-j} (s)^j [r_s]$$

$$\frac{dRe^m}{dt} = k_{fs} \sum_{j=0}^m \binom{m}{j} (-s)^j D^{m-j} - k_c Re [r_s]$$

$$\frac{d[r_s]}{dt} = k_{fs} D^0 - k_c Re^0 [r_s]$$

- Hydrogen Abstraction



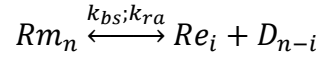
$$\frac{dD^m}{dt} = -N_H^m k_{tr,e} Re^0 (D^{m+1} - e_t D^m) + N_H^m k_{tr,e} Re^m (D^1 - e_t D^0) + N_H^e k_{tr,m} Rm^m D^0$$

$$- N_H^e k_{tr,m} Rm^0 D^m$$

$$\frac{dRe^m}{dt} = N_H^m k_{tr,e} Re^m (D^1 - e_t D^0) + N_H^e k_{tr,m} Rm^0 D^m$$

$$\frac{dRm^m}{dt} = N_H^m k_{tr,e} Re^0 (D^{m+1} - e_t D^m) + N_H^e k_{tr,m} Rm^m D^0$$

- β -Scission/Radical Addition

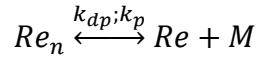


$$\frac{dRm^m}{dt} = -2k_{bs} Rm^m + k_{ra} \sum_{j=0}^m \binom{m}{j} Re^j D^{m-j}$$

$$\frac{dRe^m}{dt} = 2k_{bs} C_m Rm^m + k_{ra} Re^m D^0$$

$$\frac{dD^m}{dt} = 2k_{bs} C_m Rm^m - k_{ra} Re^0 D^m$$

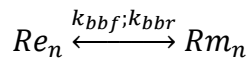
- Depropagation/Propagation



$$\frac{dRe^m}{dt} = -k_{dp} Re^m + k_p \sum_{j=0}^m \binom{m}{j} Re^{m-j} [M] + k_{dp} \sum_{j=0}^m \binom{m}{j} (-1)^j Re^{m-j} - k_p Re^m [M]$$

$$\frac{d[M]}{dt} = k_{dp} Re^0 - k_p Re^0 [M]$$

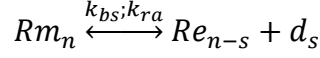
- Backbiting



$$\frac{dRe^m}{dt} = -k_{bbf}Re^m + k_{bbr}Rm^m$$

$$\frac{dRm^m}{dt} = k_{bbf}Re^m - k_{bbr}Rm^m$$

- Specific β -Scission

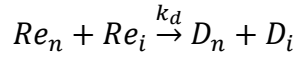


$$\frac{dRm^m}{dt} = -k_{bs}Rm^m + k_{ra} \sum_{j=0}^m \binom{m}{j} Re^{m-j}(s)^j [d_s]$$

$$\frac{dRe^m}{dt} = k_{bs} \sum_{j=0}^m \binom{m}{j} (-s)^j Rm^{m-j} - k_{ra}Re^m [d_s]$$

$$\frac{d[d_s]}{dt} = k_{bs}Rm^0 - k_{ra}Re^0 [d_s]$$

- Disproportionation



$$\frac{dD^m}{dt} = k_d Re^m Re^0 + k_d Re^0 Re^m$$

$$\frac{dRe^m}{dt} = -k_d Re^m Re^0 - k_d Re^0 Re^m$$

where the subscripts denote chain lengths in terms of the number of monomer units and the superscripts denote the moments.

The advantage of this type of modeling is directness to derive expressions for monomers of the frequency distributions. Many authors and researchers have used moment's

method as a solution for population balance equations and discussed them in great detail.

However, Mehta et al⁵⁰ pointed out that the gamma distribution cannot satisfactorily represent the initial condition. The solutions obtained from both partial differential equations and moment's method is similar but differs at long reaction times. In all cases, moment's method proves to be valid with validation done with gas permeation chromatography (GPC)^{50,53-58}.

However it requires great computational power to handle the large number of reactions.

2.4 Functional-Group, Depolymerization, Vaporization, Cross-linking Model (FG-DVC)

This model is used for modeling coal devolatilization. It combines between two models: the FG model and the DVC model. The Functional-Group (FG) model, comprised of a set of independent, first-order equations with activation energies that are distributed following a Gaussian law, is used to describe the evolution of gases while the Depolymerization, Vaporization, Cross-linking (DVC) model is used to describe the molecular weight distribution of the different fragments incorporating Monte Carlo statistical method to predict the probability of breaking and crosslinking⁵⁹. The FG-DVC model is based certain assumptions which are:

- The coal structure can be described as a cluster of rings of different sized linked into a macromolecular network
- Tar is of the same description since it is part of this network
- Coal rank does not affect kinetics
- Vapor pressure of tar fragments controls transport of escaping gases

2.5 Model findings

The variety of models used in the literature that describe the thermal and/or catalytic degradation processes differ in their degree of complexity. In this work, the literature survey findings can be summed up as follows:

- Power Law modeling is used mainly for thermogravimetric experiments and is usually not used in reactor based experimentation. It shows good fit but lacks the detail in product distribution required in advanced cases. It only tackles the kinetics of the reaction such as activation energy and rate constant.
- Lumped-Empirical modeling specifies products as gas, liquid, wax, char, or any other lump of products. It retains good fit with experimental results. However, given that it follows a pre-specified lumping scheme and that it does not give detailed carbon chain length product distribution makes it disadvantageous in that sense.
- Population-Balance based modeling surpasses the weak point of the Lumped-Empirical model and depicts a wide range of products according to carbon chain length. This is done by tracing reaction paths of the polymer chain, which is made up of thousands of monomer units, which undergo thousands of reactions. Its disadvantage, though, lies in its complexity and computational overload making it difficult to implement. Other approaches adopted include moments' method that solves the population balance equations and describes the frequency distributions of different units by relying on the first three moments and a predefined kernel. This still doesn't describe accurately the distribution of products because it relies on predefined kernels to describe the distribution.

CHAPTER 3

A TWO STAGE MODELING APPROACH FOR THE POLYETHYLENE PYROLYSIS PROCESS

The need to define product distributions and specify end products is of utmost importance when the fuel quality along with the economic, environmental, and energy aspects of the thermal degradation process are being considered. Hence the need to develop high-fidelity models that describe the frequency distribution of products is taking special attention nowadays. This work aims at developing a mechanistic model based on population balance equations that describe the mechanistic reactions that occur at the molecular level during the thermal degradation or pyrolysis of high density polyethylene. The population balance equations found in the work of Kruse et al⁵³ constitute a strong foundation for that purpose. However, unlike most models found in the literature that use the moments' method, the population balance equations are directly solved in here. This is done by combining a Lumped-Empirical model with a Population-Balance model to describe the pyrolysis process in two stages. This methodology could prove to be computationally efficient by limiting the number of equations to be solved. The characteristics of this modeling scheme are summarized as follows:

- Obtain the intermediate lumped products from polyethylene pyrolysis such as wax, low molecular weight product, and gas using a Lumped-Empirical model
- Use the intermediate lumped products from the first stage as an input to the Population-Balance model to produce the carbon chain length spectrum of the final products

The aim of this model is to combine the two models and track the product distribution according to carbon chain length within the same pyrolysis process with minimal computational effort.

3.1 Modeling the Two-Stage Pyrolysis Process

The overall pyrolysis process is comprised of two stages within the same process, being the degradation of polyethylene to a certain set of products whose lumps are predicted and the degradation of the product lumps obtained from the first stage into a set of products which are described according to their carbon chain length.

3.1.1 Modeling the First Stage

The first stage of the overall modeling process is composed of a Lumped-Empirical model to predict the various lumps of products. The model has been developed based on literature data⁶⁰. The data of low molecular weight products (Oil) and gases from Levine et al⁶⁰ have been used to construct the Lumped-Empirical model. There are missing data, however, necessary to construct the model such as the polymer and lumps profiles. For that purpose, we have assumed that the degradation profile of the lumps is similar to that found in the literature with similar degradation times². The proportionality is done by taking the Oil as a reference between two models with closely similar operating conditions and product distribution. First, the ratios of different lumps were calculated with respect to the Oil at different reaction times. Then the values of the different lumps at different reaction times were calculated with the assumption that the ratios are the same in both models since the operating conditions and product distribution are comparable.

The values are consequently calculated for the lumped model. This gives a preliminary data set in order to estimate the rate parameters for the proposed model. A parameter estimation technique was then employed to determine the parameters that involves Akaike's Final Prediction Error criterion.

The Akaike's Information Criterion (AIC) is used to estimate errors in a given data set (time series) based on unclear variations. It is an indicator of good model fit which is done by minimizing the following equation:

$$AIC = V_n \left(1 + \frac{2p}{N} \right)$$

N: number of data points

V_n: residual sum of squares

p: number of parameters in the model

The Final Prediction Error Criterion (FPE) is used to estimate the error when new model outputs are being predicted. This is done by minimizing the following equation:

$$FPE = V_n \left(1 + \frac{2p}{N - p} \right)$$

Akaike's Final Prediction Error (FPE) criterion is usually used to compare between different proposed models. Here, it is used to provide us with a good measure of the goodness of fit of the data set and the proposed model. This is done by minimizing the following equation:

$$\text{FPE} = V \left(1 + \frac{1 + \frac{d}{N}}{1 - \frac{d}{N}} \right)$$

V: loss function

d: number of estimated parameters

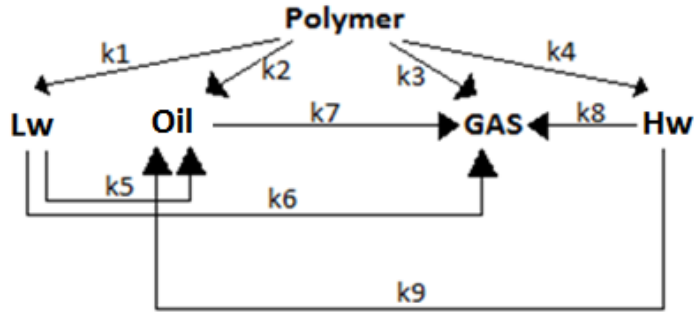
N: number of values in the estimation data set

The equation of the loss function V is as follows:

$$V = \det \left(\frac{1}{N} \sum \epsilon(t, \theta_N) (\epsilon(t, \theta_N))^T \right)$$

θ_N : estimated parameters

The proposed model involves five lumps including the polymer itself. The Polymer (P) was assumed to form low molecular weight products (Oil), gas (G), heavy wax (Hw), and Light wax (Lw). It should be noted that the Oil are those products with carbon chain length ranging from five up to twenty three. As for the wax range products, they range from a carbon chain length of twenty four up to forty four. This is because the coupling of the two models requires this division especially that the mechanistic model is based on Levine et al model⁶⁰ which depicts low molecular weight products up to a carbon chain length of twenty three. The following illustration shows the model pathways.



The governing differential equations that route this process are as follows:

$$dP/dt = -k_1P - k_2P - k_3P - k_4P$$

$$dHw/dt = k_4P - k_8Hw - k_9Hw$$

$$dLw/dt = k_1P - k_6Lw - k_5Lw$$

$$dOil/dt = k_2P + k_5Lw + k_9Hw - k_7Oil$$

$$dG/dt = k_3P + k_6Lw + k_7Oil + k_8Hw$$

P: polymer; Hw: heavy wax ranged products; Lw: light wax ranged products; Oil: lower molecular weight ranged products; G: gas ranged products.

The rate constants were, as mentioned, estimated using a grey-box modeling technique.

They are listed in the following table:

Table 4: Estimated rate constants with their corresponding standard deviations

Parameter	Value (1/min)	Standard Deviation
k1	0.170488	0.000809
k2	2.43E-08	0.000468
k3	0.0301269	0.000291
k4	0.206132	0.000964
k5	0.0146288	0.005894
k6	0.0103907	0.00589
k7	2.25E-14	0.00027
k8	0.0204982	0.004663
k9	3.48E-10	0.004665

The model was estimated from a data set with 75000 data points. The Loss function value is estimated at $4.96116e-020$ and with Akaike's FPE estimated at $4.96711e-020$.

Solving these set of differential equations using Runge-Kutta algorithm for ordinary differential equations based on the Taylor theorem yields a time distribution of the products. The rate constants were assumed to follow the Arrhenius plot and the equations to follow a first order scheme. The solution of the first stage is in excellent agreement with the literature data.

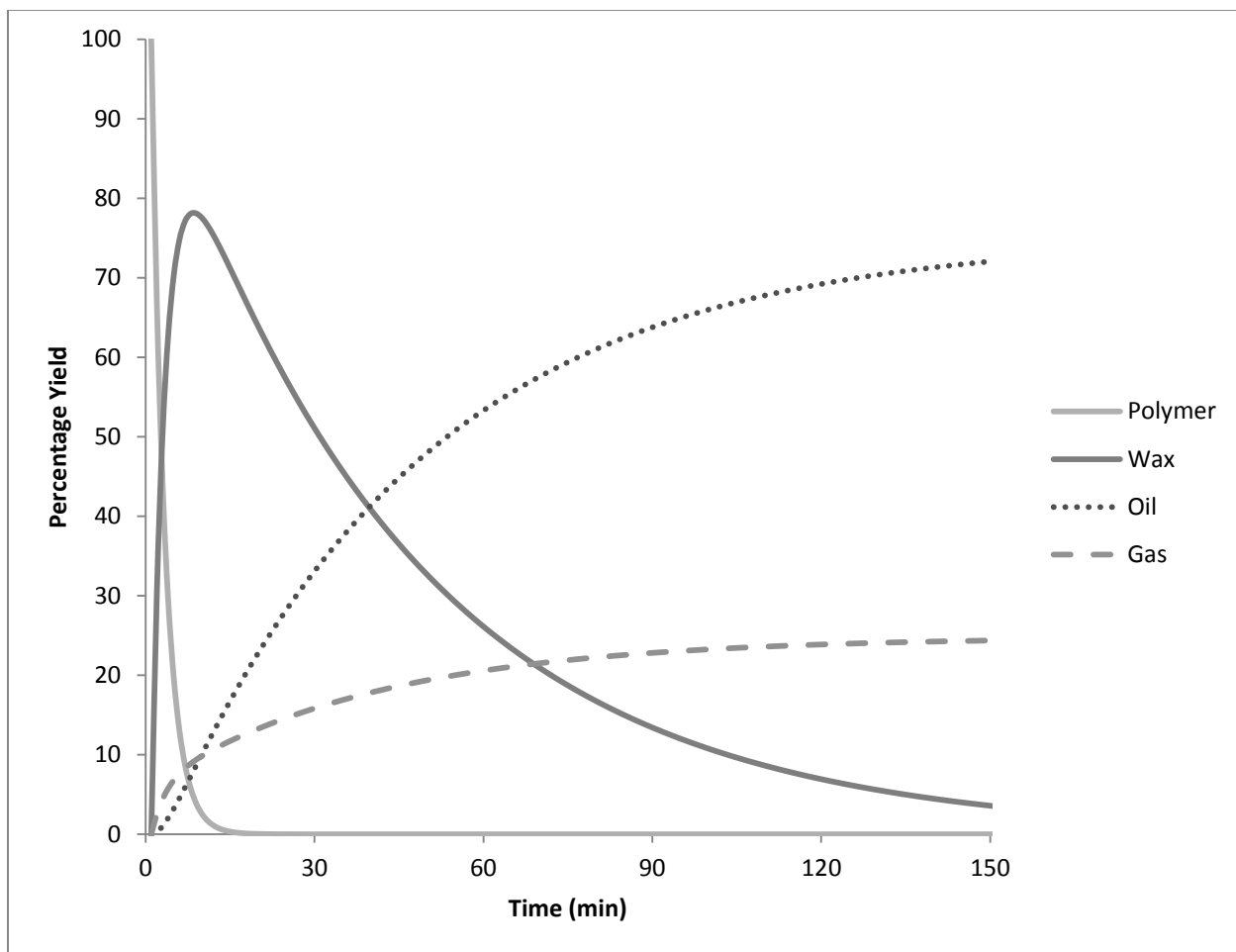


Figure 1: Time evolution of the lumps of products from the pathway model

The yield can then be easily converted to molar yield by multiplying by the total mass and dividing by the corresponding average molar mass of the lump. This gives the molar yield unit similar to that depicted in the literature⁶⁰.

3.1.2 Modeling of the Second Stage

The second stage of the pyrolysis process entails tracking the yields of the first stage model and differentiating the carbon chain length of each of the products. This is done by solving a set of differential equations which describe the population of the species. Kruse et al⁵³ developed a highly detailed mechanistic model to track product species using the moment's method to solve the population balance equations. It was imperative that the moment's method be used and to track only the first three moments due to the high number of equations involved in the reactions, which sums up to the thousands, rendering the system of equations too stiff for solving if the latter method wasn't used. This is mainly due to the fact that the number of carbon chains of polymers in general is quite large to track, ranging in the thousands. This results in a set of equations that ranges in the tens of thousands to track the large number of carbon chains of the polymer as a starting point down to the end point of the various products that range usually between one and forty carbon chain lengths. The computational demands and stiffness of the system of equations dictate that it should be reduced. This implicitly imposes the use of the moment's method as an escape from dealing with system stiffness especially that only the first three moments are required to sufficiently describe the distribution of products. Although the latter method was well proven in the literature^{49,50,55,61-66}, it does not explain some of the discrepancies between experimental and model results⁶⁰. The population balance equations in

this work were developed to be solved numerically based on the reaction mechanisms of Kruse et al ⁵³. This mechanism is the most detailed in literature, where D , Re and Rm are the dead chains, end-chain and mid-chain radicals respectively and the subscripts denote the carbon chain length with i taking any value between 1 and n , n being the maximum number of carbon chains tracked in the model. The mechanistic reactions and their corresponding population balance equations are as follows:

- Random Fission/Radical Recombination

$$D_n \xrightleftharpoons{k_f, k_c} Re_i + Re_{n-i}$$

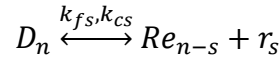
$$\frac{dD_n}{dt} = -k_f(n-1)D_n + k_c \sum_{i=1}^{n+1/2} Re_i Re_{n-i}$$

$$\frac{dRe_i}{dt} = k_f(n-1)D_n - k_c Re_i Re_{n-i}$$

$$\frac{dRe_{n-i}}{dt} = k_f(n-1)D_n - k_c Re_i Re_{n-i}$$

The dead polymer chain here can break at any point between 1 and n because of the equal probability of breakage along the chain. This results in the possibility of having random fission anywhere along the chain length. For any value of n , fission can occur at any point up to the middle of the chain, $n+1/2$, resulting in the summation to include all the possibilities of fission. Chain fission can occur for any of the products, i.e. any value of n . This requires that n be variable from the smallest chain length, here 2, up to n giving all the products the possibility to undergo chain fission. Note that the factor $n-1$ represents the number of breakable carbon chains and is used to favor the breakage of the species with higher carbon chain lengths.

- Specific Chain Fission/Radical Recombination



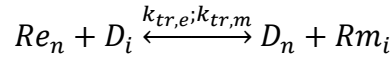
$$\frac{dD_n}{dt} = -k_{fs}(n-1)D_n + k_c Re_{n-s} r_s$$

$$\frac{dRe_{n-s}}{dt} = k_{fs}(n-1)D_n - k_c Re_{n-s} r_s$$

$$\frac{dr_s}{dt} = k_{fs}(n-1)D_n - k_c Re_{n-s} r_s$$

The dead polymer chain here can break at a specific point chosen to be a gaseous product of length 1 representing s . Specific chain fission can occur for any of the products. This requires that n be variable from the smallest chain length, here 2, up to n giving all the products the possibility to undergo specific chain fission. Note that the factor $n-1$ represents the number of breakable carbon chains and is used to favor the breakage of the species with higher carbon chain lengths.

- Hydrogen Abstraction



$$\frac{dD_i}{dt} = -N_H^m k_{tr,e} Re_n (n-1) D_i + N_H^e k_{tr,m} Rm_i D_n$$

$$\frac{dD_n}{dt} = N_H^m k_{tr,e} Re_n (n-1) D_i - N_H^e k_{tr,m} Rm_i D_n$$

$$\frac{dRe_n}{dt} = -N_H^m k_{tr,e} Re_n (n-1) D_i + N_H^e k_{tr,m} Rm_i D_n$$

$$\frac{dRm_i}{dt} = N_H^m k_{tr,e} Re_n (n-1) D_i - N_H^e k_{tr,m} Rm_i D_n$$

N_H^m and N_H^e are the number of abstractable hydrogen atoms from the mid-chain and end-chains respectively. n varies between the smallest chain length, here 3 given that we cannot have a mid-chain radical with a carbon chain length less than 3, up to n giving all the products the possibility to undergo chain fission. Note that the factor $n-1$ represents the number of breakable carbon chains and is used to favor the forward hydrogen abstraction process and formation of mid-chain radicals.

- β -Scission/Radical Addition

$$Rm_n \xrightleftharpoons[k_{ra}]{k_{bs}} Re_i + D_{n-i}$$

$$\frac{dRm_n}{dt} = -2k_{bs}Rm_n + k_{ra} \sum_{i=1}^{n+1/2} Re_i D_{n-i}$$

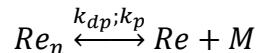
$$\frac{dRe_i}{dt} = 2k_{bs}Rm_n - k_{ra}Re_i D_{n-i}$$

$$\frac{dD_{n-i}}{dt} = 2k_{bs}Rm_n - k_{ra}Re_i D_{n-i}$$

The free electron on the mid-chain radical could reside anywhere along the chain length except for the ends of the chain. This results in the possibility of having β -Scission anywhere along the chain length. For any value of n , β -Scission can occur at any point up to the middle of the chain, $n+1/2$, resulting in the summation to include all the possibilities of scissions. Because the

minimum number of carbon atoms for a mid-chain radical is 3, n varies from the latter up to n to fully include all the species that can undergo β -Scission.

- Depropagation/Propagation



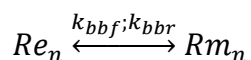
$$\frac{dRe_n}{dt} = -k_{dp}Re_n + k_pReM$$

$$\frac{dRe}{dt} = k_{dp}Re_n - k_pReM$$

$$\frac{dM}{dt} = k_{dp}Re_n - k_pReM$$

Monomer formation in depropagation is straight forward and can occur at any chain length thus the variation of n should be between 3, the smallest chain length to yield a monomer, up to n .

- Backbiting



$$\frac{dRe_n}{dt} = -k_{bbf}Re_n + k_{bbr}Rm_n$$

$$\frac{dRm_n}{dt} = k_{bbf}Re_n - k_{bbr}Rm_n$$

Although this is a reaction not resulting in a change of carbon chain length, it consists of several reactions of hydrogen shifts. End-chain hydrogen shifts include 1-4, 1-5, 1-6, and 1-7 and mid-

chain hydrogen shifts include $x-x+3$, $x-x+4$, $x-x+5$ where x is the position of the free electron on the product chain.

- Specific β -Scission/Radical Addition

$$Rm_n \xrightleftharpoons{k_{bs};k_{ra}} Re_{n-s} + d_s$$

$$\frac{dRm_n}{dt} = -k_{bs}Rm_n + k_{ra}Re_{n-s}d_s$$

$$\frac{dRe_{n-s}}{dt} = k_{bs}Rm_n - k_{ra}Re_{n-s}d_s$$

$$\frac{dd_s}{dt} = k_{bs}Rm_n - k_{ra}Re_{n-s}d_s$$

The mid-chain radical undergoes scission at a specific point chosen to be a gaseous product of length 4 representing s . Specific β -Scission can occur for any of the products. This requires that n be variable from the smallest chain length, here 5 due to the size of the chosen product, up to n giving all the products the possibility to undergo specific β -Scission.

- Disproportionation

$$Re_n + Re_i \xrightarrow{k_d} D_n + D_i$$

$$\frac{dD_n}{dt} = k_d Re_n Re_i$$

$$\frac{dD_i}{dt} = k_d Re_n Re_i$$

$$\frac{dRe_n}{dt} = -k_d Re_n Re_i$$

$$\frac{dRe_i}{dt} = -k_d Re_n Re_i$$

This termination reaction can cover all the range of products thus requiring n to vary between 1 and n .

The rate constants for the former reactions follow the Arrhenius law and were adopted from the literature^{60,62}. They are listed in the table below.

Table 5: Rate parameters for mechanistic reactions' rate constants

Reaction Type	Symbol	Frequency factor, A (1/s or L/(mol.s))	Intrinsic barrier, E0 (kcal/mol)	Transfer coefficient	Delta_Heat of reaction (kcal/mol)	Activation Energy (kcal/mol)
Chain fission	kf	1E+16	2.3	1	87.36	89.66
Allyl chain fission	kfs	1E+16	2.3	1	72.9	75.2
Radical recombination	kc	1.1E+11	2.3	0	-87.36	2.3
Disproportionation	kd	1.10E+10	2.3	0	NA	2.3
End-chain b-scission	kdp	1.32E+13	11.4	0.76	22.35	28.386
End-chain b-scission backwards	kp	1.32E+13	11.4	0.76	22.35	28.386
Mid-chain b-scission	kbsm	5.35E+14	11.4	0.76	23.03	28.9028
b-scission to LMWS	kbsl	2.33E+13	11.4	0.76	22.97	28.8572
Radical addition	kra	2.88E+07	11.4	0.24	-23.03	5.8728
Hydrogen abstraction forward	ktre	2.75E+08	12	1	-1.57	10.43
Hydrogen abstraction backward	ktrm	2.75E+08	12	1	-1.57	10.43
1,4-hydrogen shift	kbbRe1_4	1.58E+11	NA	NA	NA	20.8
1,5-hydrogen shift	kbbRe1_5	1.82E+10	NA	NA	NA	13.7
1,6-hydrogen shift	kbbRe1_6	1.05E+10	NA	NA	NA	18.3
1,7-hydrogen shift	kbbRe1_7	3.00E+09	NA	NA	NA	18.3
x,x+3-hydrogen shift	kbbRmx_x3	1E+11	NA	NA	NA	21.2
x,x+4-hydrogen shift	kbbRmx_x4	1.26E+11	NA	NA	NA	14.7
x,x+5-hydrogen shift	kbbRmx_x5	7.24E+09	NA	NA	NA	18.1

NA: not available

3.1.2.1 Product Yields from the Second Stage Model

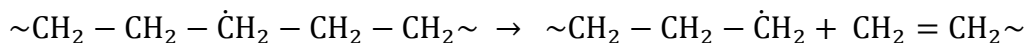
The mechanistic reactions of the Population-Balance model are involved in the bond-breaking and the formation of radicals to various products. Different reactions account for different product formation. They can be summarized in the table below:

Table 6: Product formation from different reaction types

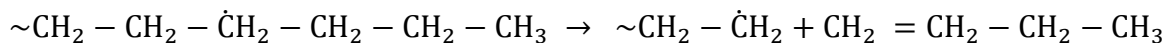
Reaction Type	Product Formed
Random Fission	End-chain Radical
Specific Chain Fission	Mid-chain Radical
Radical Recombination	Single-bond Product
Hydrogen Abstraction	Single-bond Product and Mid-chain Radical
β -Scission	Double-bond Product and End-chain Radical
Specific β -Scission	Double-bond Product and End-chain Radical
Radical Addition	Mid-chain Radical
Depropagation	Double-bond Product and End-chain Radical
Propagation	End-chain Radical
Backbiting	Mid-chain Radical (forward); End-chain Radical (backward)
Disproportionation	Single-bond Product and Double-bond Product

The product yields of the second stage model differentiate between single-bond and double-bond products. It should be noted that double-bond products are formed with the following mechanistic reactions:

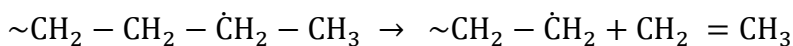
- β -Scission



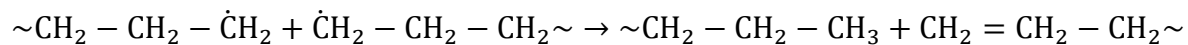
- Specific β -Scission



- Depropagation



- Disproportionation



The former set of differential equations was developed specifically with the intention of solving them numerically in conjunction with the pathway model.

CHAPTER 4

MODEL ASSEMBLY AND SOLUTION

4.1 Model Assembly

The combined model is designed to work in a consecutive manner, solving each model at a time. The pathway model is solved with the purpose of delivering the proper initial conditions for the mechanistic model. Although the pathway model is depicted for the whole degradation period, being 150 minutes as shown in the previous chapter, the values of the lumps are taken at the time where the yield of the polymer is near negligible (0.01 percent). This is due to the fact that the mechanistic model does not make use of the values of the polymer because of its high carbon chain length that ranges in the thousands. As discussed before, this renders the system of equations too stiff for solving. However, the values of the other lumps of products from the pathway model are used as input for the mechanistic model with yields of the pathway model evenly distributed according to the lump's carbon chain length range. The assumption of even distribution for the products was done based on literature data and after sensitivity analysis was carried out. The best fit was that coinciding with the even distribution of carbon-chain products according to their corresponding lumps. This means that the yield of the Oil, which contains carbon-chain products ranging from five up to twenty three, is divided equally over its nineteen products. The same applies to the other lumps of waxes and gas.

Wax-range products are considered to be the highest carbon-chained products in this model. They include products up to 44 carbon-chains according to the literature⁶⁷ as well as our own analysis using GC/MS of waxy products from HDPE pyrolysis at 420°C. Therefore, the

mechanistic model tracks forty four carbon chain lengths to their final set of products constituted of single and double bonds. The species are tracked via two sets of differential equations, one following a first order scheme for the pathway model, and the other described by a set of differential algebraic equations constituting a stiff system.

The pathway model was solved using Runge-Kutta algorithm for ordinary differential equations based on the Taylor theorem while the mechanistic model was solved using numerical differentiation formulas, due to the size and complexity of the function to be differentiated.

The combined model tracked 181 species. The following assumptions were adopted:

- Isothermal conditions for the entire reaction time
- Even spatial distribution for the polymer melt
- Relatively small time and reaction scales allowing species to react before they leave the polymer melt

4.2 Model Solution

The model tracked two sets of products. One is lumped set and the other is the carbon-chain set. The first set of products is depicted for 24 minutes which is the time where the polymer has a negligible value of 0.01 percent. This is crucial in the model solution because the mechanistic model is only tracking the concentrations of the lumps, after being evenly distributed as an initial condition, whereby the latters are composed of carbon chain length of up to forty four. This is also very important to limiting the number of equations to be solved and thus making the system of equations of the mechanistic model overall less stiff and thus less computationally demanding. The illustrations below show a comparison between the model

results and literature experimental results of Levine et al⁶⁰ for a carbon-chain length range between 8 and 23, similar to that depicted in the literature.

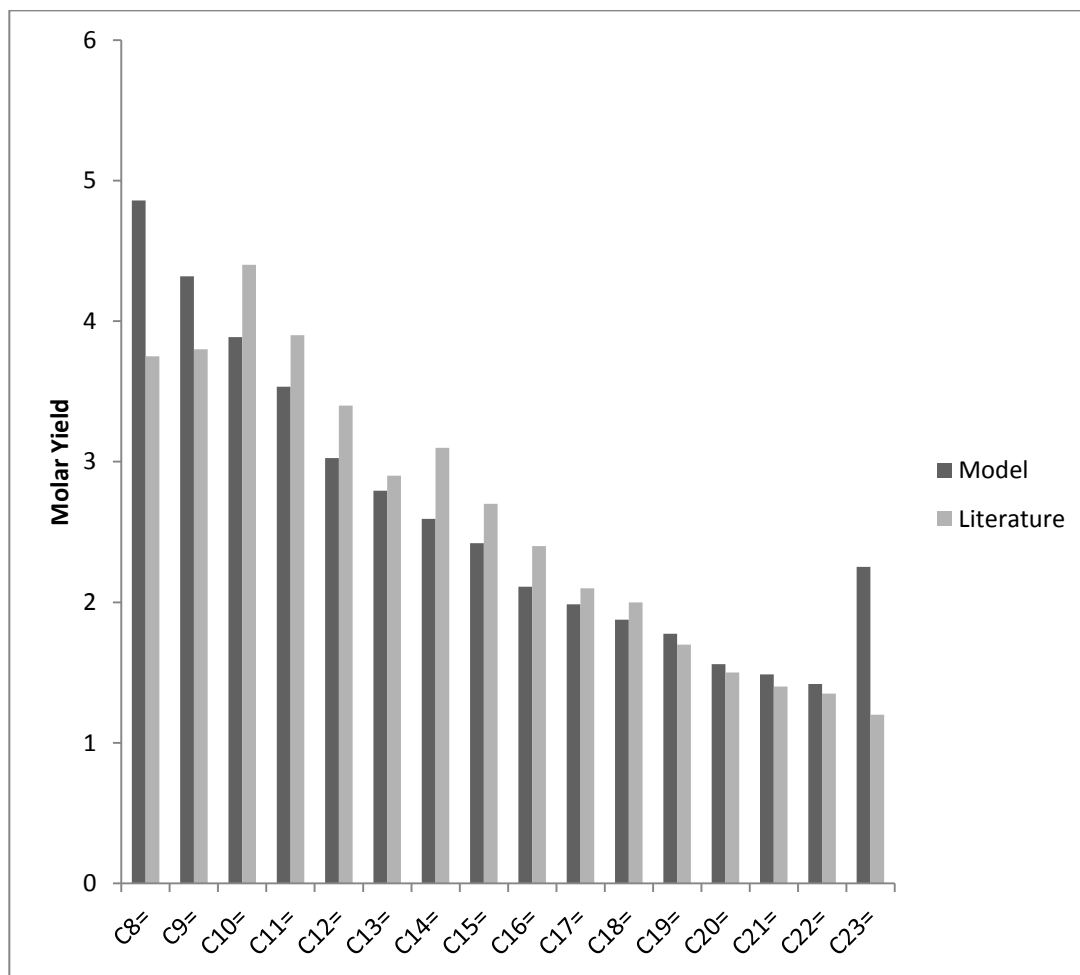


Figure 2: Comparison between model and literature results of condensable alkene yields for 125,000 M_{w0} HDPE pyrolysis at 420 °C after 90 minutes

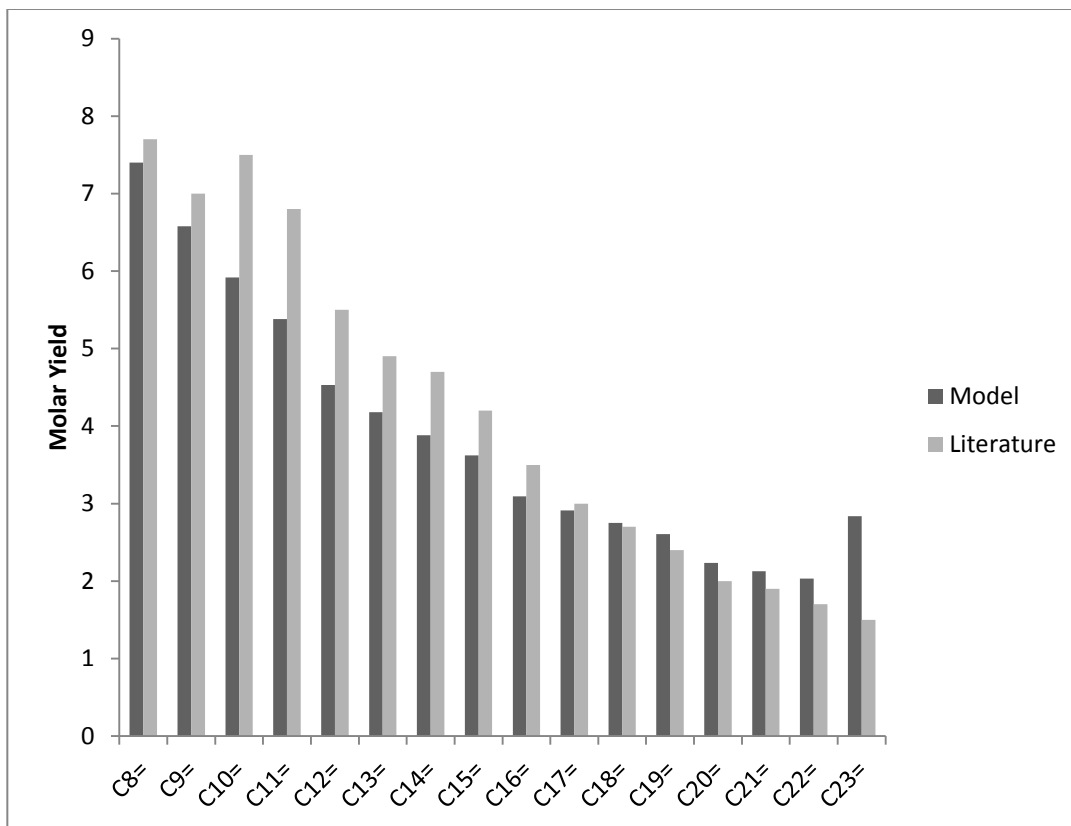


Figure 3: Comparison between model and literature results of condensable alkene yields for 125,000 M_{w0} HDPE pyrolysis at 420 °C after 150 minutes

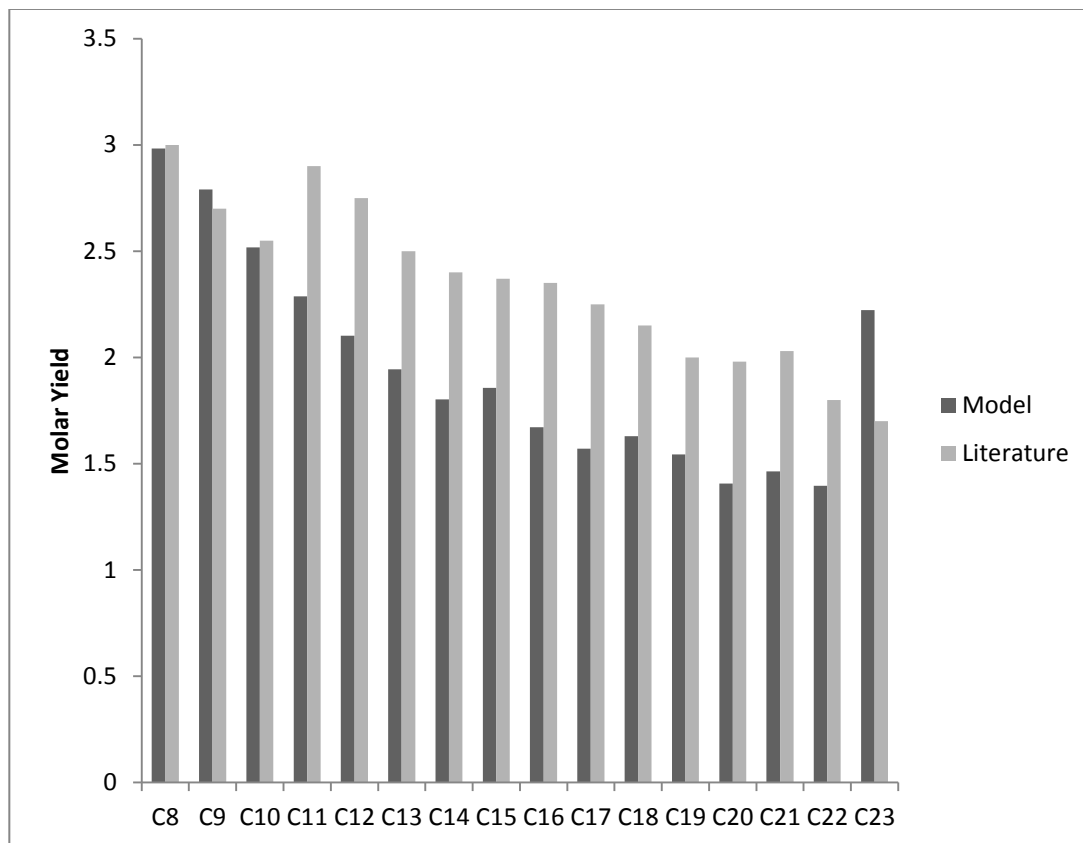


Figure 4: Comparison between model and literature results of condensable alkane yields for 125,000 M_{w0} HDPE pyrolysis at 420 °C after 90 minutes

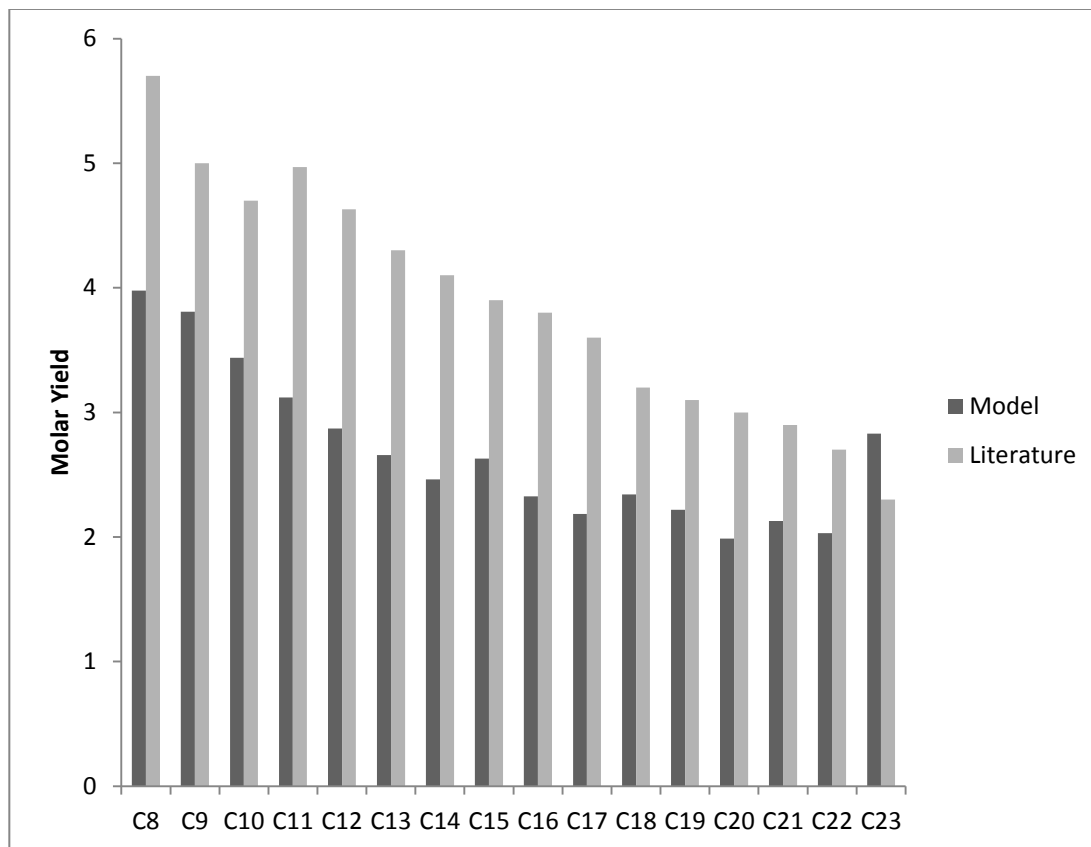


Figure 5: Comparison between model and literature results of condensable alkene yields for 125,000 M_{w0} HDPE pyrolysis at 420 °C after 150 minutes

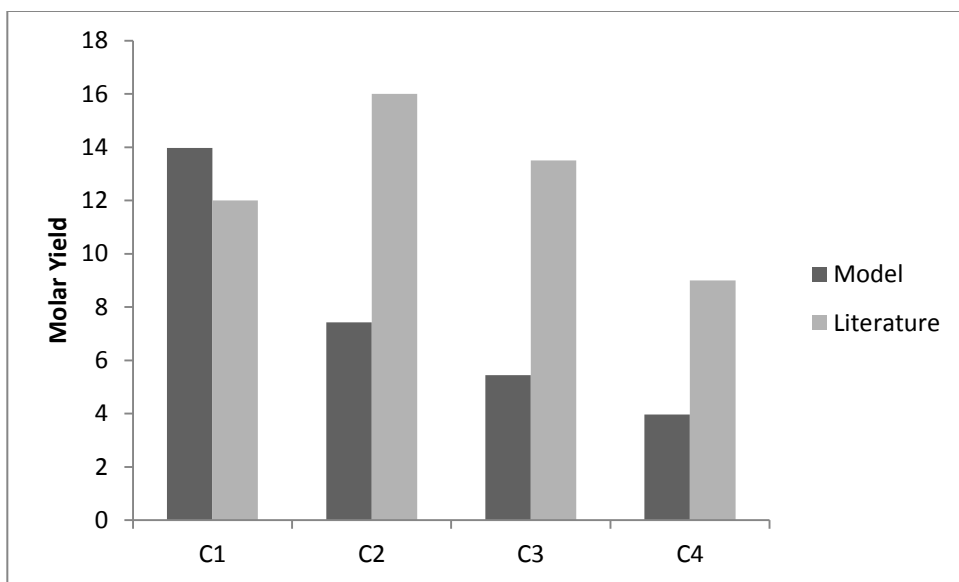


Figure 6: Comparison between model and literature results of gaseous alkane yields for 125,000 M_{w0} HDPE pyrolysis at 420 °C after 90 minutes

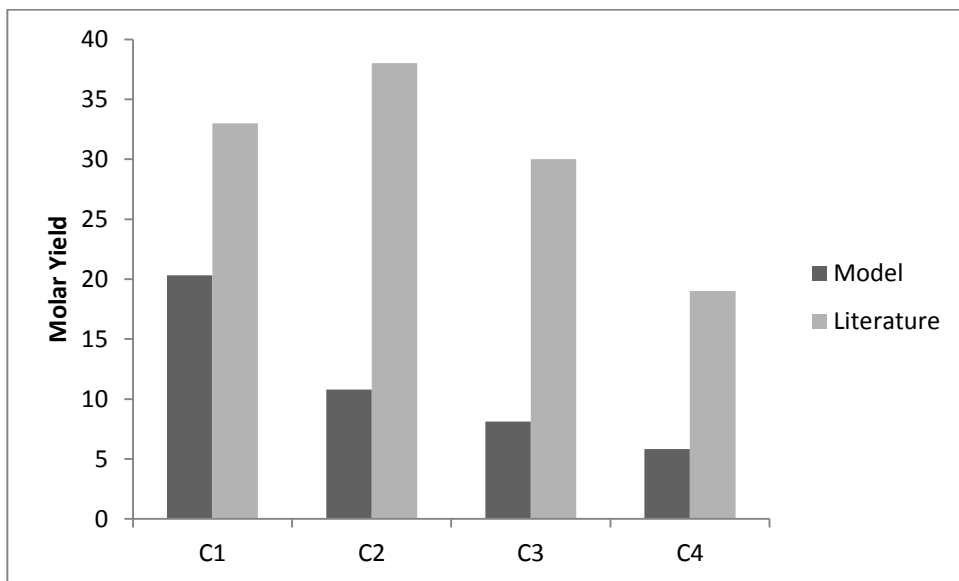


Figure 7: Comparison between model and literature results of gaseous alkane yields for 125,000 M_{w0} HDPE pyrolysis at 420 °C after 150 minutes

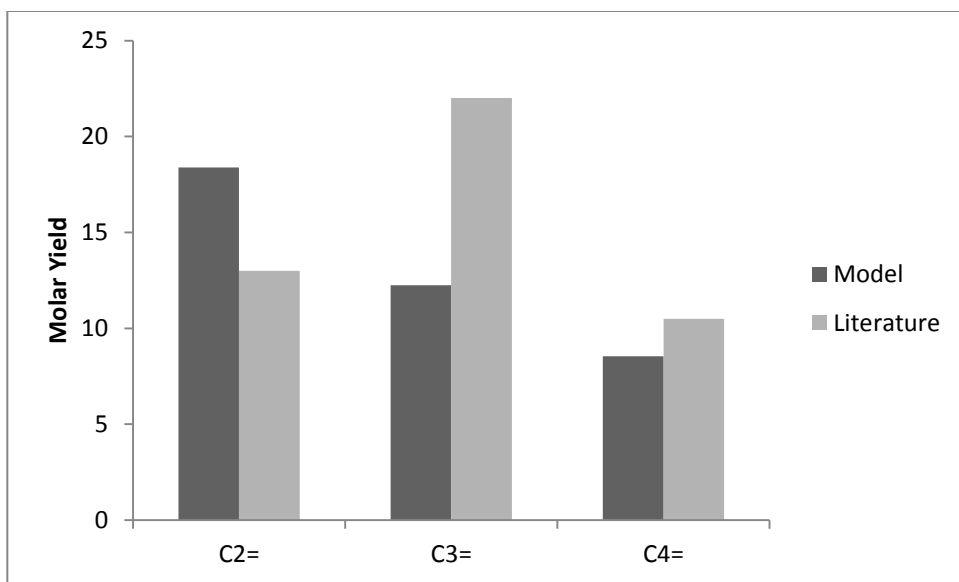


Figure 8: Comparison between model and literature results of gaseous alkene yields for 125,000 M_{w0} HDPE pyrolysis at 420 °C after 90 minutes

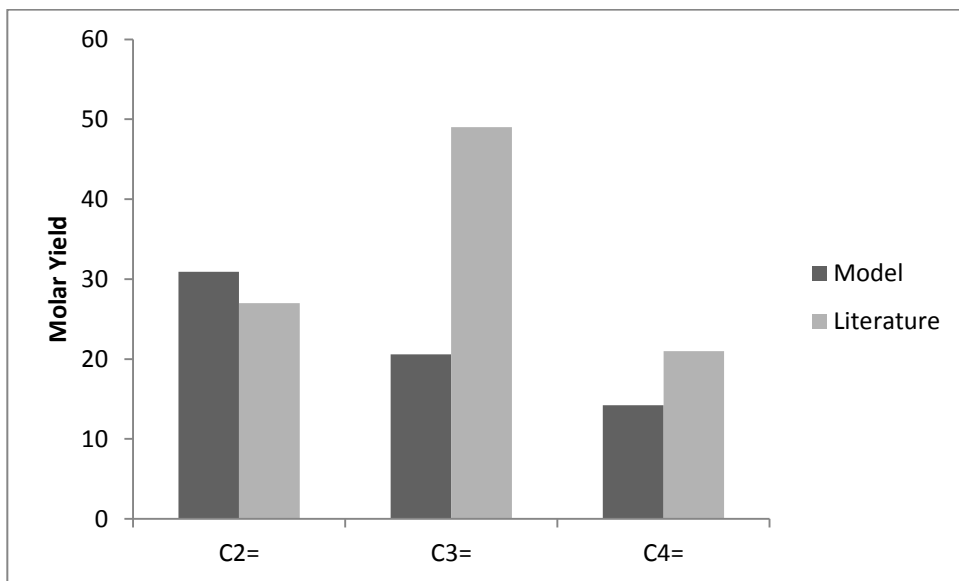


Figure 9: Comparison between model and literature results of gaseous alkene yields for 125,000 M_{w0} HDPE pyrolysis at 420 °C after 150 minutes

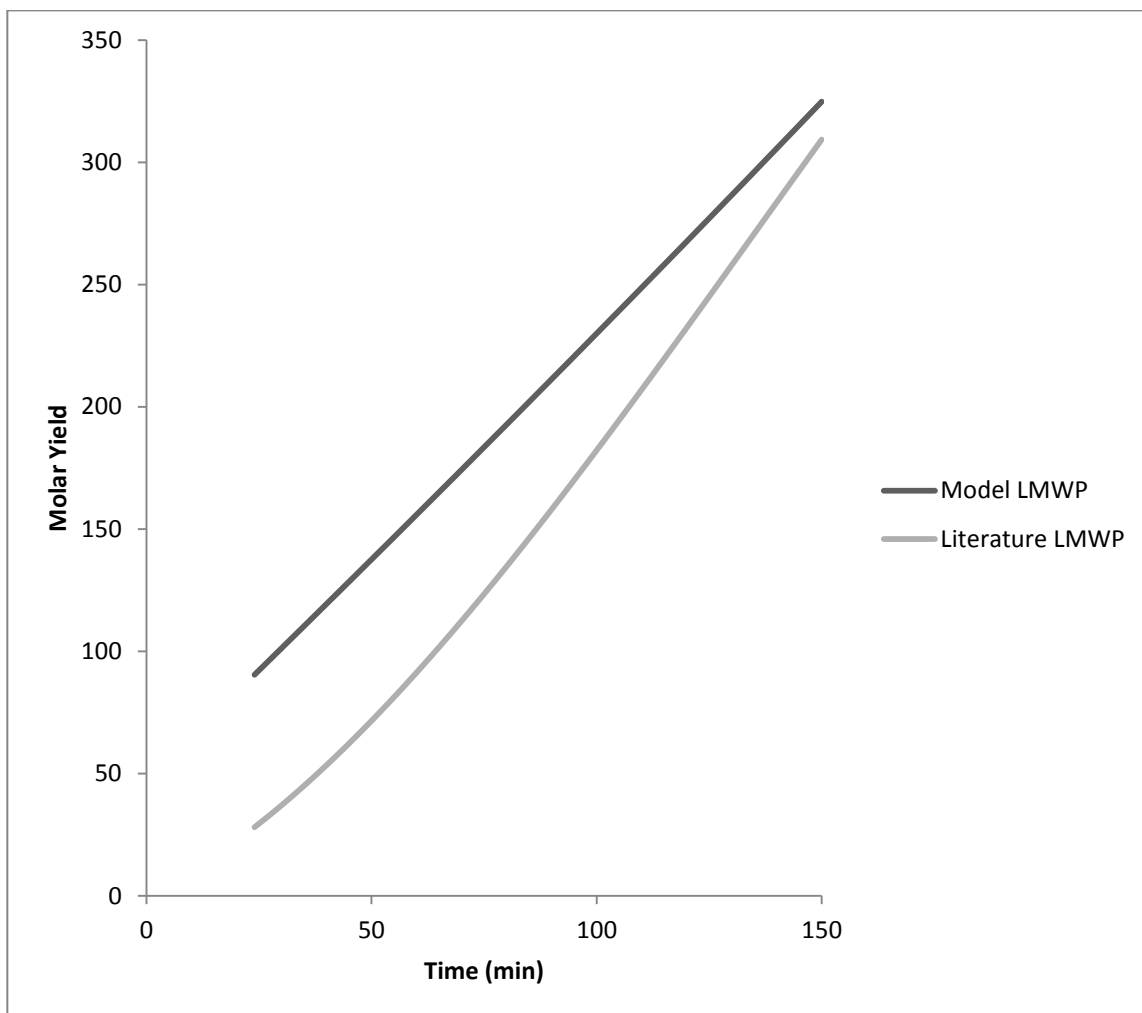


Figure 10: Comparison between model and literature time evolution results of Oil yields for 125,000 M_{w0} HDPE pyrolysis at 420 °C

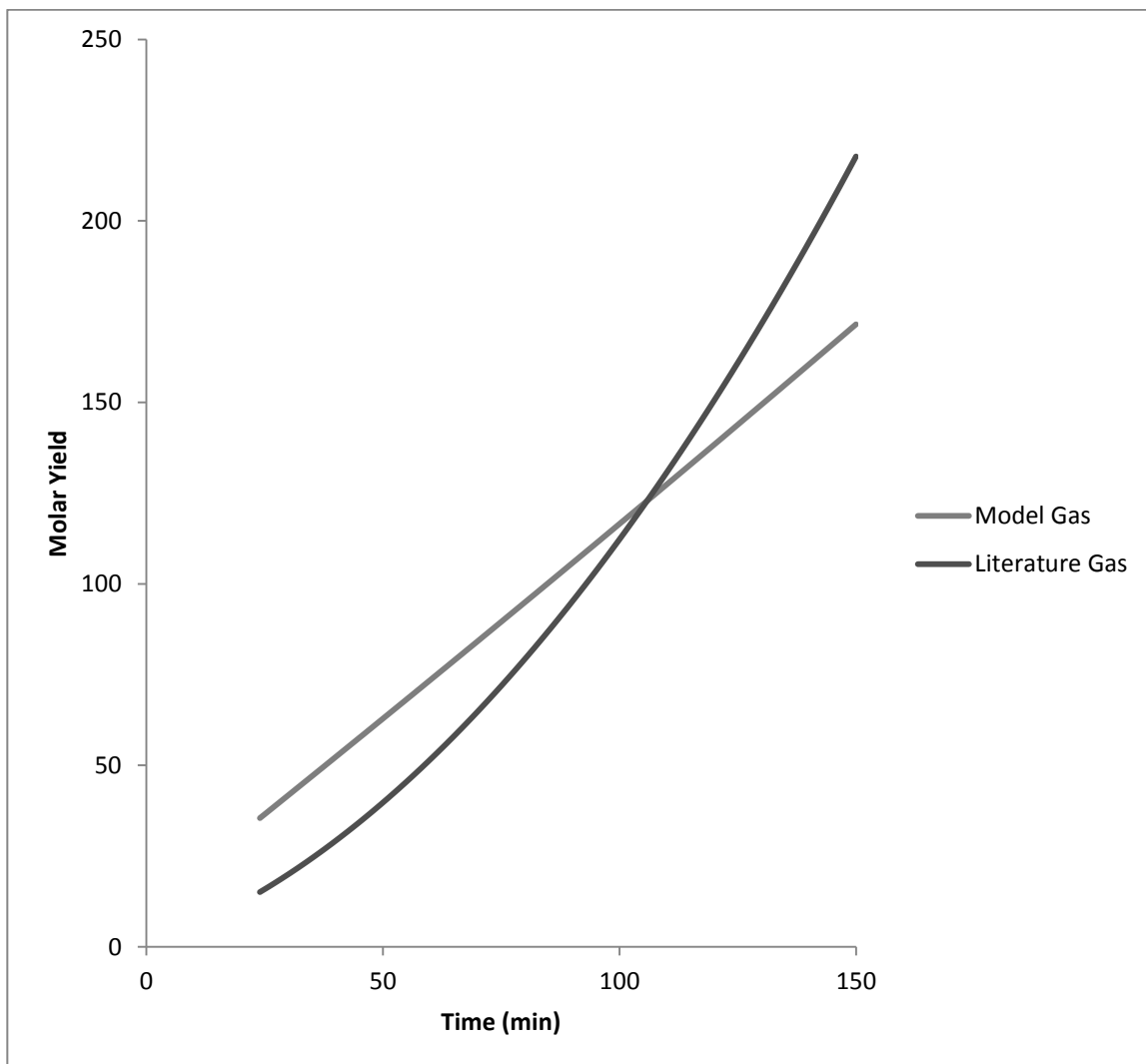


Figure 11: Comparison between model and literature time evolution results of Gas yields for 125,000 M_{w0} HDPE pyrolysis at 420 °C

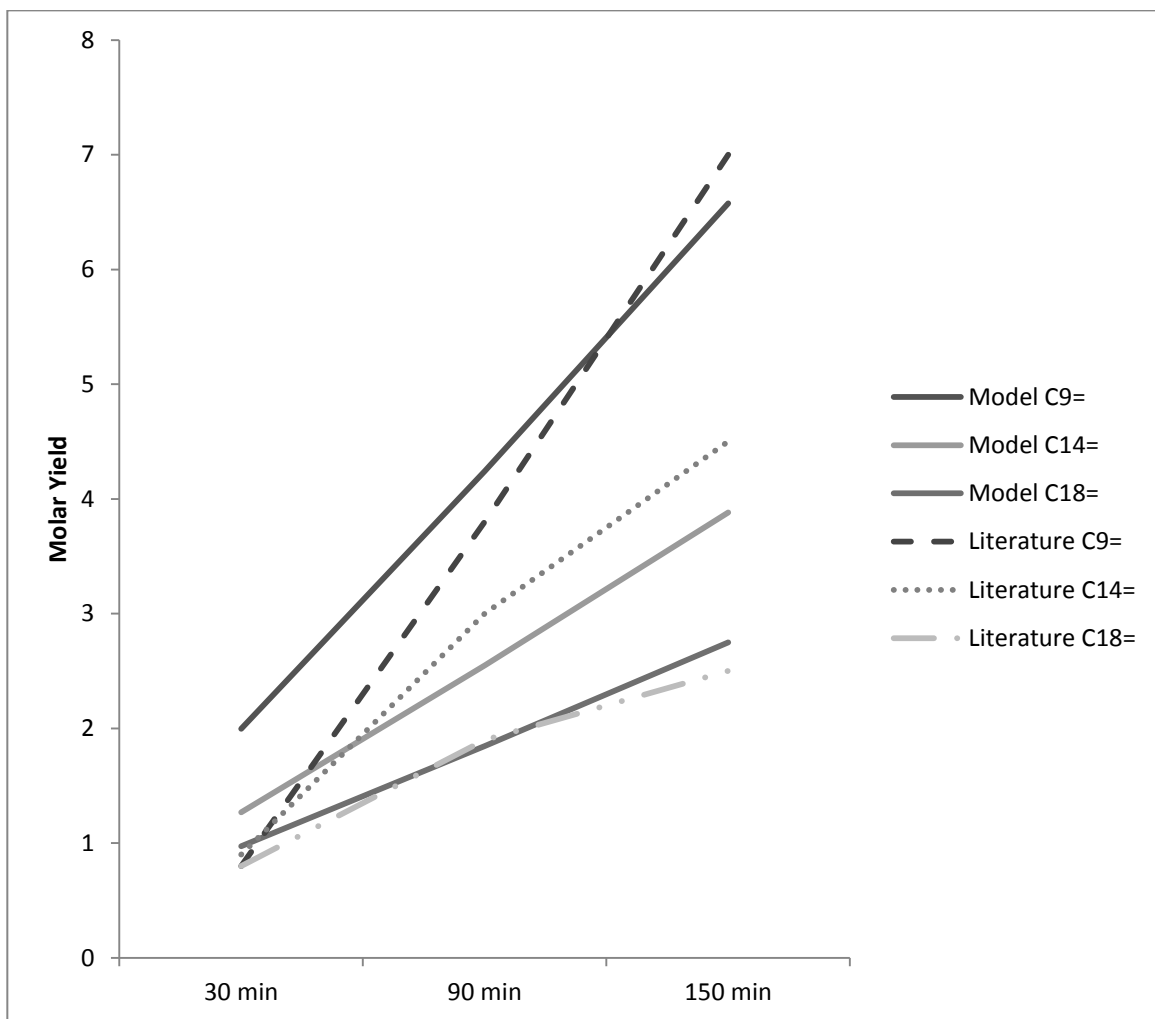


Figure 12: Comparison between model and literature time evolution results for =C₉, =C₁₄ and =C₁₈ for 125,000 M_{w0} HDPE pyrolysis at 420 °C

4.3 Discussion

The results of the condensable alkanes and alkenes fit quite well with the literature experimental results. It is evident that the results of the double-bonded products are more closely matched to the literature data than their single-bonded counterparts. This can be attributed to two factors. One is the initial condition provided by the pathway model and the other would be the lack of structural tracking such as branching, cyclization and aromatization. The pathway model fits well with the literature data given. However, the evolutions of the lumps of products follow a profile typical of that of a first order system as seen in the literature⁶⁸. Also, the lack of data for the other lumps of Hw and Lw, which were assumed, made the pathway model assembly more difficult to mimic the results of Oil and gases. This made the initial condition that were entered into the mechanistic model slightly different from the data provided by Levine et al⁶⁰.

Nonetheless, the results closely match the literature data giving a novel method to track individual products, both single and double bonds, in a very low computationally demanding manner. As for the effects of branching, cyclization and aromatization, they are evident in the gas data. The molar yields of C₂= and C₄= are comparable to the literature. The single-bonded gaseous products are not predicted accurately. The same reason for the discrepancy is also applicable here as with the condensable products. The time evolution of the Oil and gases fit well with the literature data.

The model adopted the same mechanistic reactions as the literature^{55,60}, thus, does not have a different approach to the mechanistic aspect of the solution to getting the product evolution. Rather, it approaches the solution in a different way than what is offered in the literature which is tracking the detailed products only after the initial polymer has been transformed into lower molecular weight products (e.g. wax, oil and gas) in order not to be

included in the set of mechanistic equations for the purpose of limiting them, making them less computationally demanding which is the main objective of this work.

The model tracks mid-chain and end-chain radicals. This was important for explaining the evolution of the products as well as their behavior. It was also essential for the solution of the mechanistic model. Moreover, the model indicated that the presence of both mid-chain and end-chain radicals is at most times 84 percent of the overall mix of products. This means that as the reaction proceeds and the polymer starts to undergo different mechanistic reactions starting with the random fission reaction, the presence of mid-chain and end-chain radicals is dominant. Little is known about the behavior of radicals in a pyrolysis process, except for their very high rate of formation and transformation to dead polymers. This model offers, for the first time in the literature, a new insight on radical presence in a pyrolysis process. This is quite important for future development of pyrolysis processes, especially in the case a new technology for radical handling arises. Although some results of this model are not comparable with literature data, it has been justified by further development of the model relating to branching, cyclization and aromatization as well as the pathway model order; it forms a springboard for future development of this new approach to solving a pyrolysis detailed mechanistic model.

CHAPTER 5

CONCLUSIONS AND RECOMMENDATIONS

5.1 Conclusions

A new approach was introduced to model polymer pyrolysis. A combined model was developed comprising of a Lumped-Empirical (pathway) model and a Population-Balance (mechanistic) model. The two models were established for this work based on data from the literature^{53,60}. The pathway model consisted of five lumps of products including the polymer. Not all data for the lumps were readily available; therefore, some of the time evolution of lumps, as well as rate parameters, was estimated using a grey-box modeling technique which had good fit with the literature data. This was employed as part of a two-stage model whereby the output of this model was set as input for the second-stage which is the Population-Balance or mechanistic model. The population balance equations, developed based on the work of Kruse et al⁵³, that describe the mechanistic reactions were solved numerically here rather than using the traditional moments' method that is widely used in the literature. This was possible due to the coupling of the two models which enabled tracking a low carbon-chain length product-range rather than the very high carbon-chain length of the polymer. It enabled the model to be highly efficient despite adopting a numerical solution rather than a moments' method to solve the population balance equations that describe the mechanistic reactions that take place during the pyrolysis process. The combined model tracked 181 species for HDPE, with 125,000 M_{w0} , pyrolysis at 420 °C. The model displayed very good fit for the condensable alkanes and alkenes and a fair fit for the

gaseous products. The discrepancy in some of the results, especially the gaseous products, can be attributed to further needed development of the model.

5.2 Recommendations

The following recommendations can be made to further develop this modeling work:

- Develop a pathway model with no missing data. Although this work has a good fit with the literature, it could be further enhanced with more data at hand.
- Adopt a higher order modeling scheme for the pathway model since the low number of equations that describe this process permits a more complex model to be adopted without compromising computational efficiency. This will set a better initiation point for the second-stage model and thus, a better overall fit.
- Include structural characteristics of the polymer such as branching and weak bonds. These characteristics affect the final product yield and thus, provide a better fit.
- Include cyclization and aromatization reactions that take place during the pyrolysis process. This would further enhance the fit of the final products.

REFERENCES

- (1) Aguado, J.; Serrano, D. P. *Feedstock Recycling of Plastic Wastes*; ROYAL SOCIETY OF CHEMISTRY, 1999.
- (2) Aguado, J.; Serrano, D. P.; Escola, J. M. *Industrial & Engineering Chemistry Research* **2008**, *47*, 7982–7992.
- (3) Aguado, J.; Serrano, D. P. *Feedstock Recycling of Plastic Wastes*; 1999.
- (4) Stivala, S. *Applied Science: London* **1983**.
- (5) Wampler, T. P. In *Applied Pyrolysis Handbook, Second Edition*; 2007; pp. 1–26.
- (6) Abbot, J. *Journal of Catalysis* **1987**, *107*, 451–462.
- (7) Murata, K. *Journal of Analytical and Applied Pyrolysis* **2009**, *86*, 354–359.
- (8) Uemichi, Y.; Nakamura, J.; Itoh, T.; Sugioka, M.; Garforth, A. a.; Dwyer, J. *Industrial & Engineering Chemistry Research* **1999**, *38*, 385–390.
- (9) Lin, H.-T.; Huang, M.-S.; Luo, J.-W.; Lin, L.-H.; Lee, C.-M.; Ou, K.-L. *Fuel Processing Technology* **2010**, *91*, 1355–1363.
- (10) Lin, Y.; Yang, M. *Polymer Degradation and Stability* **2009**, *94*, 25–33.
- (11) Serrano, D.; Aguado, J.; Rodriguez, J.; Peral, a *Journal of Analytical and Applied Pyrolysis* **2007**, *79*, 456–464.
- (12) Elordi, G.; Olazar, M.; Lopez, G.; Artetxe, M.; Bilbao, J. **2011**.
- (13) Marcilla, A.; Beltran, M.; Navarro, R. *Journal of Analytical and Applied Pyrolysis* **2005**, *74*, 361–369.
- (14) López, a; de Marco, I.; Caballero, B. M.; Adrados, a; Laresgoiti, M. F. *Waste management (New York, N.Y.)* **2011**, *31*, 1852–8.
- (15) Songip, A. R.; Masuda, T.; Kuwahara, H.; Hashimoto, K. *Energy & Fuels* **1994**, *8*, 136–140.
- (16) Schirmer, J.; Kim, J. S.; Klemm, E. **2001**, *60*, 205– 217.
- (17) Valde, F. *Chemical Engineering* **2007**, *79*, 433–442.

- (18) Aguado, J.; Serrano, D. P.; Miguel, G. S.; Escola, J. M.; Rodríguez, J. M. *Journal of Analytical and Applied Pyrolysis* **2007**, *78*, 153–161.
- (19) Marcilla, A. *Polymer* **2001**, *42*, 8103–8111.
- (20) Marcilla, A. *Polymer Degradation and Stability* **2003**, *80*, 233–240.
- (21) Marcilla, A. *Journal of Analytical and Applied Pyrolysis* **2002**, *64*, 85–101.
- (22) Doyle, C. D. *Journal of Applied Polymer Science* **1961**, *5*, 285–292.
- (23) Friedman, H. L. *Journal of Polymer Science Part C: Polymer Symposia* **1964**, *6*, 183–195.
- (24) Coats, A. W.; Redfern, J. P. *Nature* **1964**, *201*, 68–69.
- (25) Flynn, J. H.; Wall, L. A. *Journal of Polymer Science Part B: Polymer Letters* **1966**, *4*, 323–328.
- (26) Ozawa, T. *Bulletin of the Chemical Society of Japan* **1965**, 707.
- (27) Kissinger, H. E. *Analytical Chemistry* **1957**, *29*, 1702–1706.
- (28) Akahira, T.; Sunose, T. *Research Report Chiba Institute Technology* **1971**.
- (29) Brems, A.; Baeyens, J.; Beerlandt, J.; Dewil, R. *Resources, Conservation and Recycling* **2011**, *55*, 772–781.
- (30) Grammelis, P.; Basinas, P.; Malliopoulou, A.; Sakellaropoulos, G. *Fuel* **2009**, *88*, 195–205.
- (31) Marcilla, A.; Beltran, M.; Conesa, J. a. *Journal of Analytical and Applied Pyrolysis* **2001**, *58-59*, 117–126.
- (32) Marcilla, A.; Gomez, A.; Reyeslabarta, J.; Giner, A.; Hernandez, F. *Journal of Analytical and Applied Pyrolysis* **2003**, *68-69*, 467–480.
- (33) Encinar, J. M.; González, J. F. *Fuel* **2008**, *9*, 12–14.
- (34) Gao, Z. *Polymer Degradation and Stability* **2003**, *81*, 125–130.
- (35) Sánchez-Jiménez, P. E.; Pérez-Maqueda, L. a.; Perejón, A.; Criado, J. M. *Polymer Degradation and Stability* **2010**, *95*, 733–739.
- (36) Westerhout, R. W. J.; Waanders, J.; Kuipers, J. a. M.; van Swaaij, W. P. M. *Industrial & Engineering Chemistry Research* **1997**, *36*, 1955–1964.

- (37) Aboulkas, a.; El harfi, K.; El Bouadili, a. *Energy Conversion and Management* **2010**, *51*, 1363–1369.
- (38) Marongiu, a.; Bozzano, G.; Dente, M.; Ranzi, E.; Faravelli, T. *Journal of Analytical and Applied Pyrolysis* **2007**, *80*, 325–345.
- (39) Songip, Ahmad Rahman; Masuda, Takao Masuda; Kuwahara, Hiroshi; Hashimoto, K. *Energy* **1994**, 131–135.
- (40) Elordi, G.; Lopez, G.; Olazar, M.; Aguado, R.; Bilbao, J. *Journal of Hazardous Materials* **2007**, *144*, 708–714.
- (41) Al-Salem, S. M.; Lettieri, P. *Chemical Engineering Research and Design* **2010**, *88*, 1599–1606.
- (42) Miskolczi, N.; Bartha, L.; Deak, G.; Jover, B.; Kallo, D. *Process Safety and Environmental Protection* **2004**, *82*, 223–229.
- (43) Lin, Y.-H. *Polymer Degradation and Stability* **2009**, *94*, 1924–1931.
- (44) Lin, Y.-H.; Yang, M.-H.; Wei, T.-T.; Hsu, C.-T.; Wu, K.-J.; Lee, S.-L. *Journal of Analytical and Applied Pyrolysis* **2010**, *87*, 154–162.
- (45) Costa, P.; Pinto, F.; Ramos, a. M.; Gulyurtlu, I.; Cabrita, I.; Bernardo, M. S. *Energy & Fuels* **2010**, *24*, 6239–6247.
- (46) Faravelli, T. *Journal of Analytical and Applied Pyrolysis* **2001**, *60*, 103–121.
- (47) Faravelli, T. *Journal of Analytical and Applied Pyrolysis* **1999**, *52*, 87–103.
- (48) Faravelli, T. *Journal of Analytical and Applied Pyrolysis* **2003**, *70*, 761–777.
- (49) Madras, G.; Chung, G. Y.; Smith, J. M.; McCoy, B. J. *Industrial & Engineering Chemistry Research* **1997**, *36*, 2019–2024.
- (50) Mehta, K.; Madras, G. *AIChE Journal* **2001**, *47*, 2539–2547.
- (51) Sterling, W. J.; McCoy, B. J. *AIChE Journal* **2001**, *47*, 2289–2303.
- (52) Himmelblau, D. M.; Bischoff, K. B. *Process Analysis and Simulation: Deterministic Systems*; Wiley (New York), 1968; pp. 192–199.
- (53) Kruse, T. M.; Woo, O. S.; Wong, H.-W.; Khan, S. S.; Broadbelt, L. J. *Macromolecules* **2002**, *35*, 7830–7844.
- (54) Kruse, T. M.; Wong, H.-W.; Broadbelt, L. J. *Macromolecules* **2003**, *36*, 9594–9607.

- (55) Kruse, T. M.; Wong, H.-W.; Broadbelt, L. J. *Industrial & Engineering Chemistry Research* **2003**, *42*, 2722–2735.
- (56) Kruse, T.; Levine, S.; Wong, H.; Duoss, E.; Lebovitz, A.; Torkelson, J.; Broadbelt, L. *Journal of Analytical and Applied Pyrolysis* **2005**, *73*, 342–354.
- (57) Sezgi, N. A.; Cha, W. S.; Smith, J. M.; McCoy, B. J. *Industrial & Engineering Chemistry Research* **1998**, *37*, 2582–2591.
- (58) Madras, G.; Smith, J.; McCoy, B. J. *Industrial & engineering chemistry research* **1996**, *35*, 1795–1800.
- (59) Serio, P. R. S. M. A.; Yu, D. G. H. Z. Z. ADVANCES IN THE FG-DVC MODEL OF COAL DEVOLATILIZATION. *Advanced Fuel Research*.
- (60) Levine, S. E.; Broadbelt, L. J. *Polymer Degradation and Stability* **2009**, *94*, 810–822.
- (61) McCoy, B. J. *Chemical engineering science* **1996**, *51*, 2903–2908.
- (62) Kruse, T. M.; Woo, O. S.; Wong, H.-W.; Khan, S. S.; Broadbelt, L. J. *Macromolecules* **2002**, *35*, 7830–7844.
- (63) McCoy, Y. K. W. S. C. B. J. 1003–1007.
- (64) Marongiu, a; Faravelli, T.; Ranzi, E. *Journal of Analytical and Applied Pyrolysis* **2007**, *78*, 343–362.
- (65) Madras, G. *Polymer Degradation and Stability* **1997**, *58*, 131–138.
- (66) McCoy, B. J.; Madras, G. *Chemical Engineering Science* **2001**, *56*, 2831–2836.
- (67) Morrison, R.; Boyd, R. *Organic Chemistry*; 6th ed.; 1993.
- (68) Costa, P. A.; Pinto, F. J.; Ramos, A. M.; Gulyurtlu, I. K.; Cabrita, I. A.; Bernardo, M. S. *Energy* **2007**, 2489–2498.